medRxiv preprint doi: https://doi.org/10.1101/2025.02.13.25322003; this version posted February 14, 2025. The copyright holder for this preprint (which was not certified by peer review) is the author/funder, who has granted medRxiv a license to display the preprint in perpetuity. All rights reserved. No reuse allowed without permission.

Pathological expansion of gut microbiome-associated *Enterococcus* in advanced cirrhosis corresponds with multilevel perturbations of the gut-liver-immune axis

Authors

Matthew J Dalby[1,2], Raymond Kiu[1,2], Marilena Stamouli[3], Betsy Arefaine[3], Lex E X Leong[4], Jack Hales[5], Christine Bernsmeier[6,7], Arjuna Singanayagam[8], Sidsel Støy[9], Maria-Emanuela Maxan[3,6], Merianne Mohamad[3], Ane Zamalloa[6], Matt Lewis[10], Royce P. Vincent[11,12], Roger Williams[17], Lindsey A Edwards[6], Shilpa Chokshi[3,13], Mark Thursz[10,14], Naiara Beraza[5], Charalambos G Antoniades[10], Geraint B Rogers[4], Julia A Wendon[3], Kenneth D Bruce[15], Debbie L Shawcross[3], Mark JW McPhail[3,6,10], Lindsay J Hall[1,2,5,16*], Vishal C Patel[3,6*]

Affiliations

1. Department of Microbes, Infection & Microbiomes, School of Infection, Inflammation and Immunology, College of Medicine & Health, University of Birmingham, Birmingham, UK.
2. Institute of Microbiology & Infection, University of Birmingham, Birmingham, UK.
3. Roger Williams Institute of Liver Studies, School of Immunology & Microbial Sciences, Faculty of Life Sciences and Medicine, King's College London, Foundation for Liver Research and King's College Hospital, London, UK
4. Infection & Immunity Theme, South Australian Health & Medical Research Institute, North Terrace, Adelaide, SA, Australia.
5. Food, Microbiome and Health, Quadram Institute Bioscience, Norwich Research Park, Norwich, UK.
6. Institute of Liver Studies, King's College Hospital NHS Foundation Trust, London, United Kingdom
7. Department of Biomedicine, University of Basel, Switzerland.
8. Infection Clinical Academic Group, St. George's School of Health and Medical Sciences, City St. George's University of London, Cranmer Terrace, London, SW17 0RE, UK.
9. Department of Hepatology and Gastroenterology, Aarhus University Hospital, DK-8200 Aarhus, Denmark.
10. Division of Digestive Disease, Department of Metabolism, Digestion & Reproduction, Imperial College London, London, UK.
11. Department of Clinical Biochemistry, King's College Hospital NHS Foundation Trust, London, UK;
12. Department of Nutritional Sciences, Faculty of Life Sciences and Medicine, King's College London, London, UK
13. Faculty of Health, University of Plymouth, Devon, UK.

NOTE: This preprint reports new research that has not been certified by peer review and should not be used to guide clinical practice.

medRxiv preprint doi: https://doi.org/10.1101/2025.02.13.25322003; this version posted February 14, 2025. The copyright holder for this preprint (which was not certified by peer review) is the author/funder, who has granted medRxiv a license to display the preprint in perpetuity. All rights reserved. No reuse allowed without permission.

14. Imperial College Healthcare NHS Trust, St Mary's Hospital, Praed St, London, UK.
15. Institute of Pharmaceutical Science, King's College London, UK.
16. Norwich Medical School, University of East Anglia, Norwich Research Park, Norwich, UK.
17. *In memoriam.*
* Joint last and corresponding authors.

Keywords: Cirrhosis; Liver failure; Microbiota: *Enterococcus*; Bile acids

Funding statement: The observational study was adopted to the National Institute for Health Research (NIHR) Clinical Research Network (CRN) portfolio, supporting participant screening and recruitment by the Liver Research and Anaesthetics, Critical Care, Emergency and Trauma Teams at King's College Hospital NHS Foundation Trust. VCP was supported by a New Investigator Award from the Intensive Care Foundation (Registered charity number: 2940178) and Clinical Research Network South London Principal Investigator Strategic "GreenShoot" Research Delivery and Development Funding. The clinical trial was funded through an investigator-initiated study grant awarded by Norgine Pharmaceuticals UK Limited to King's College London. Infrastructure to support the trial was also provided by the Medical Research Council (MRC) Centre for Transplantation, King's College London, UK – MRC grant no. MR/J006742/1. Laboratory assays were also part funded by a generous donation from a Liver Service User to the King's College Hospital Institute of Liver Studies and Transplantation Charity Research Fund, King's College Hospital Charity (Registered charity number: 1165593). MS, BA, MEM, MM, SC and VCP were supported and bioinformatic analyses were part funded by the Foundation for Liver Research (Registered charity number: 268211/1134579). LJH is supported by Wellcome Trust Investigator Award (220876/Z/20/Z); the Biotechnology and Biological Sciences Research Council (BBSRC), Institute Strategic Programme Gut Microbes and Health (BB/R012490/1), and its constituent projects BBS/E/F/000PR10353 and BBS/E/F/000PR10356, and the BBSRC Institute Strategic Programme Food, Microbiome and Health BB/X011054/1 and its constituent project BBS/E/QU/230001B. MT Acknowledges support from the NIHR-Imperial Biomedical Research Centre and the Medical Research Council Precision Medicine Award (MR/R014019/1).

medRxiv preprint doi: https://doi.org/10.1101/2025.02.13.25322003; this version posted February 14, 2025. The copyright holder for this preprint (which was not certified by peer review) is the author/funder, who has granted medRxiv a license to display the preprint in perpetuity. All rights reserved. No reuse allowed without permission.

Conflicts of interest:

VCP has undertaken consultancy for Norgine Pharmaceuticals Ltd, Alfasigma S.p.A. and Menarini Diagnostics Ltd.

DLS has undertaken consultancy for Norgine Pharmaceuticals Ltd, EnteroBiotix, MRM Health, Apollo Therapeutics, Genfit and Satellite Biosciences.

RPV reports Honoraria from Novo Nordisk, Amarin UK and AstraZeneca.

AS has delivered paid lectures for Bristol Myers Squibb.

MD, LH, RK, GR, SS, SC, KB, MJWM have no conflicts.

Authors contributions:

- Matthew J Dalby: Data curation, Formal analysis, Investigation, Software, Visualisation, Writing - Original Draft, Writing - Review & Editing
- Raymond Kiu: Data curation, Formal analysis, Writing - Review & Editing
- Marilena Stamouli: Data curation, Formal analysis, Writing - Review & Editing
- Betsy Arefaine: Data curation, Formal analysis
- Lex E X Leong: Data curation, Formal analysis, Investigation, Visualization, Writing - Review & Editing
- Jack Hales: Methodology, Writing - Review & Editing
- Christine Bernsmeier: Data curation, Formal analysis, Visualization, Writing - Review & Editing
- Arjuna Singanayagam: Data curation, Formal analysis, Visualization, Writing - Review & Editing
- Sidsel Støy: Data curation, Formal analysis, Visualization, Writing - Review & Editing
- Maria-Emanuela Maxan: Data curation, Writing - Review & Editing
- Merianne Mohamad: Visualization, Writing - Review & Editing
- Matt Lewis: Investigation, Methodology, Writing - Review & Editing
- Royce P Vincent: Resources, Writing - Review & Editing
- Roger Williams: Supervision
- Lindsey A Edwards: Data curation, Formal analysis, Writing - Review & Editing
- Shilpa Chokshi: Supervision, Writing – review & editing

medRxiv preprint doi: https://doi.org/10.1101/2025.02.13.25322003; this version posted February 14, 2025. The copyright holder for this preprint (which was not certified by peer review) is the author/funder, who has granted medRxiv a license to display the preprint in perpetuity. All rights reserved. No reuse allowed without permission.

- Mark Thursz: Resources, Supervision, Writing – review & editing
- Naiara Beraza: Investigation, Resources, Writing - Review & Editing
- Charalambos G Antoniades: Supervision
- Geraint B Rogers: Conceptualisation, Data curation, Formal analysis, Investigation, Resources, Supervision, Visualization, Writing - Review & Editing
- Julia A Wendon: Conceptualisation, Supervision, Writing – review & editing
- Kenneth D Bruce: Conceptualisation, Supervision, Writing – review & editing
- Debbie L Shawcross: Conceptualisation, Funding acquisition, Project administration, Resources, Supervision, Writing – review & editing, served as Chief Investigator of RIFSYS Trial
- Mark JW McPhail: Conceptualisation, Formal analysis, Supervision, Writing - Review & Editing
- Vishal C Patel: Conceptualisation, Funding acquisition, Investigation, Methodology, Project administration, Resources, Supervision, Writing – review & editing, served as Chief Investigator of GLA study
- Lindsay J Hall: Conceptualisation, Funding acquisition, Investigation, Methodology, Project administration, Resources, Supervision, Writing – review & editing

Data availability:

The 16S rRNA amplicon sequencing raw reads are deposited in NCBI SRA under project PRJNA1223169.

medRxiv preprint doi: https://doi.org/10.1101/2025.02.13.25322003; this version posted February 14, 2025. The copyright holder for this preprint (which was not certified by peer review) is the author/funder, who has granted medRxiv a license to display the preprint in perpetuity. All rights reserved. No reuse allowed without permission.

Abstract

Background: Chronic liver disease (CLD) is a progressive condition that, in its advanced stages, leads to cirrhosis with related clinical complications, and can lead to acute-on-chronic liver failure (ACLF) - a syndrome marked by critical illness, multi-organ dysfunction and high mortality. Systemic inflammation in ACLF can occur without overt infection, indicating alternative pathways of immune activation and microbial translocation. Intestinal perturbations, bacterial translocation, and the resulting systemic inflammation and immune dysfunction are defining features of ACLF, yet the identification of specific microbial contributors remains poorly elucidated.

Objective: To investigate the relationship between gut microbiome alterations, systemic inflammation, and clinical markers of disease severity across the cirrhosis spectrum.

Design: This cross-sectional, prospective study analysed faecal microbiota, plasma bile acids, urinary and plasma metabolites, markers of gut and systemic inflammation and translocation, and monocyte dysfunction, in a well-phenotyped cohort of patients with ACLF, decompensated cirrhosis and stable cirrhosis, in comparison with healthy individuals.

Results: Advanced stages of cirrhosis were marked by a higher abundance of *Enterococcus*, which correlated with markers of systemic inflammation, particularly in ACLF patients. Concurrently, the abundance of anaerobic commensal genera such as *Roseburia*, *Ruminococcus*, and *Faecalibacterium* were significantly lower. Lower urinary hippurate and trimethylamine N-oxide TMAO levels, linked to reduced microbial metabolism and dietary fibre intake, paralleled these microbiome changes. While elevated plasma primary bile acids reflected hepatic dysfunction, systemic inflammatory markers suggested parallel gut barrier dysfunction and microbial translocation in advanced cirrhosis.

Conclusion: This study underscores a potential role of greater intestinal *Enterococcus* abundance, as cirrhosis severity increases and where clinically there is more antibiotic exposure, as a driver of gut barrier inflammation and dysfunction, and systemic immune dysfunction in advanced cirrhosis. Further research into tailored microbiome-targeted therapies, including prebiotics and probiotics,

medRxiv preprint doi: https://doi.org/10.1101/2025.02.13.25322003; this version posted February 14, 2025. The copyright holder for this preprint (which was not certified by peer review) is the author/funder, who has granted medRxiv a license to display the preprint in perpetuity. All rights reserved. No reuse allowed without permission.

and more focused antibiotic use may prevent *Enterococcus* dominance and restore gut-liver axis homeostasis and mitigate disease progression in CLD.

Key messages

What is already known on this topic:

- CLD can progress to ACLF, a life-threatening syndrome with high mortality rates characterised by systemic inflammation, impaired phagocytosis and immune dysfunction with associated multiple organ failure.
- The gut microbiome's role in underpinning the gut-liver axis is recognised, with microbial perturbations and gut barrier dysfunction associated with CLD, yet the exact microbiome changes and their link to inflammatory pathways remain unclear.

What this study adds:

- This study reveals that *Enterococcus* significantly increases with CLD severity and antibiotic use and correlates with markers of systemic inflammation and gut barrier dysfunction.
- Reductions in obligate anaerobe commensal bacteria, such as *Roseburia* and *Faecalibacterium*, are observed, alongside depressed levels of key microbial metabolites, including hippurate and TMAO, across CLD stages.
- These changes suggest that *Enterococcus* predominance and gut microbiome perturbations driven by factors including disease severity and antibiotic use may actively drive inflammation and impaired monocyte function in CLD.

How this study might affect research, practice, or policy:

- Findings indicate that *Enterococcus* and wider gut microbiome perturbations provide a rationale for targeting as therapeutic strategies to modulate the gut-liver axis in CLD.

medRxiv preprint doi: https://doi.org/10.1101/2025.02.13.25322003; this version posted February 14, 2025. The copyright holder for this preprint (which was not certified by peer review) is the author/funder, who has granted medRxiv a license to display the preprint in perpetuity. All rights reserved. No reuse allowed without permission.

- This highlights the potential of microbiome-focused interventions, such as faecal microbial transplantation, probiotics, prebiotics or phages, to improve gut health, reduce gut and systemic inflammation, and ultimately mitigate cirrhosis-related complications.
- Future research and development of targeted microbiome therapeutics may positively influence CLD management including a focus on antimicrobial stewardship, and inform clinical guidelines whilst improving patient outcomes.

medRxiv preprint doi: https://doi.org/10.1101/2025.02.13.25322003; this version posted February 14, 2025. The copyright holder for this preprint (which was not certified by peer review) is the author/funder, who has granted medRxiv a license to display the preprint in perpetuity. All rights reserved. No reuse allowed without permission.

1. Introduction

Chronic liver disease (CLD) is a progressive condition, resulting from several different aetiologies such as alcohol, viral hepatitis, and obesity that can culminate in cirrhosis and eventual liver failure (Huang et al., 2023). An important aspect of CLD is the development of acute-on-chronic liver failure (ACLF), a distinct syndrome characterised by multi-organ dysfunction, worsening liver function, and liver failure, with high mortality rates (Katoonizadeh et al., 2010; Moreau et al., 2013; Shah et al., 2024). The transition to decompensated cirrhosis, preceding ACLF, can lack identifiable triggers, confounding therapeutic options, exacerbating morbidity, and reducing transplant-free survival (D'Amico et al., 2022; Trebicka et al., 2021).

The gut microbiota is a key component of the 'gut-liver axis' but its interplay with the disease mechanisms is still not fully understood in CLD (Albillos et al., 2020; Hsu and Schnabl, 2023). While bacterial infections can act as a trigger of progression to ACLF, many cases (60-70%) display systemic inflammation without identifiable infection, with 50% of patients with 'sepsis' culture negative, suggesting alternative inflammatory pathways and limitations in infection diagnosis methods (Hernaez et al., 2017; Toledo et al., 1993). This 'sterile inflammation' in CLD patients may be driven by damage-associated molecular patterns (DAMPs) released from stressed or dying hepatocytes particularly in those without clear triggers such as active alcohol use or culture-confirmed bacterial infections (Arroyo et al., 2015). Additionally, translocation of viable bacteria or microbial components (i.e. microbial-associated molecular patterns [MAMPs]) via a dysfunctional intestinal barrier, may contribute to systemic inflammation, precipitating cirrhosis-related complications. Increased markers of gut permeability and inflammation in CLD patients further support the link between microbial translocation and inflammatory responses (Alexopoulou et al., 2017).

The gut microbiota potentially plays a dual role in CLD, serving as a reservoir for pathogens and MAMPs, while also simultaneously maintaining gut homeostasis through its resident commensal bacteria (Adak and Khan, 2019; Caballero-Flores et al., 2023). These commensal microbes are critical for gut epithelial integrity, pathobiont exclusion (and preventing overgrowth), and metabolite

medRxiv preprint doi: https://doi.org/10.1101/2025.02.13.25322003; this version posted February 14, 2025. The copyright holder for this preprint (which was not certified by peer review) is the author/funder, who has granted medRxiv a license to display the preprint in perpetuity. All rights reserved. No reuse allowed without permission.

production (e.g. short-chain fatty acids [SCFAs]) essential for host health (Ghosh et al., 2021). In CLD, however, gut microbiota disruptions are frequently observed, associated with reduced intestinal barrier integrity, leading to increased microbial translocation. This process introduces intestinal bacteria and MAMPs into the systemic circulation, contributing to cirrhosis-related inflammation, particularly in advanced disease stages. Studies in CLD have reported reductions in commensal bacterial genera such as *Ruminococcus, Faecalibacterium, Bacteroidetes,* and *Coprococcus* (Da Silva et al., 2018; Dubinkina et al., 2017), accompanied by increases in pathobiont taxa like *Enterococcaceae*, *Staphylococcaceae*, and *Enterobacteriaceae* (Bajaj et al., 2014). Additionally, patients with CLD show altered bile acid homeostasis, characterised by alterations in bile acid quantities and composition, which correlate with microbiota shifts and reduced conversion of primary to secondary bile acids (Kakiyama et al., 2013; Mouzaki et al., 2016), with more primary bile acids being found in faeces (Kakiyama et al., 2014). These changes, mirrored in serum bile acids, worsen with cirrhosis progression (Horvatits et al., 2017). However, comprehensive studies integrating microbiota alterations to systemic metabolites, inflammatory and gut barrier markers, across CLD stages remain limited. (Bajaj et al., 2022, 2014, 2012).

This study aimed to identify alterations in bacterial genera in the faecal microbiota, as targets for future therapeutic intervention, across a well-phenotyped cohort of patients with ACLF, decompensated cirrhosis, stable cirrhosis, and healthy controls. We aimed to understand some of the potential functional properties in these microbiome changes by comparison with profiling of serum bile acids, urinary and plasma metabolites, and markers of gut inflammation, bacterial translocation and systemic immune activation, as key pathobiological processes within the gut-liver-immune axis. We hypothesised that microbiota perturbations increase with CLD severity. By correlating these microbiota differences with relevant metabolic, inflammatory, immunological and clinical disease markers, we aimed to detect key target bacteria within the gut that are associated with disruption within the gut-liver-immune axis, providing insights into disease pathobiology and informing potential therapeutic targets.

medRxiv preprint doi: https://doi.org/10.1101/2025.02.13.25322003; this version posted February 14, 2025. The copyright holder for this preprint (which was not certified by peer review) is the author/funder, who has granted medRxiv a license to display the preprint in perpetuity. All rights reserved. No reuse allowed without permission.

3. Results

3.1 Participant characteristics

This cross-sectional cohort included patients with cirrhosis who were categorised based on disease stage and severity; stable cirrhosis (SC), decompensated cirrhosis (DC), or acute-on-chronic liver failure (ACLF). A healthy control (HC) group of healthy participants was included for comparison analysis and to establish normal values. Table 1 summarises demographic, clinical and biochemical characteristics of the recruited patients and healthy controls. A total of 153 patients with cirrhosis were included in this study (SC=15, DC=81, ACLF=57) with 40 HCs. Patients with cirrhosis were older than HC with a mean HC age of 38 years (SD: 10 years) and mean liver cohort age of 53 years (SD: 11 years). Predominant aetiologies of cirrhosis included alcohol-related liver disease (ARLD) (SC/DC/ACLF: 60%/70.4%/57.9%) and metabolic- dysfunction associated steatotic liver disease (MASLD) (SC/DC/ACLF: 20%/8.6%/10.5%), respectively. SC, DC and ACLF patients presented with ascites (33.3%/71.6%/96.5%) and HE (6.7%/43.2%/86%) as predominant manifestations of hepatic decompensation, respectively. None of the cirrhosis patients had experienced a variceal haemorrhage in the 7 days prior to recruitment nor had spontaneous bacterial peritonitis at the time of sampling. DC and ACLF patients were more frequently receiving antibiotics acutely 45.7%/91.2%, respectively) compared to SC (20%). There was no difference in use of rifaximin-α (only five participants received rifaximin-α monotherapy as antibiotic treatment), lactulose, non-selective beta-blockers and acid suppression therapies (proton pump inhibitors, H2 antagonists) across the cirrhosis cohorts. Haematological, biochemical and disease severity and prognostic composite scores followed expected patterns. Transplant-free survival at 90 days was 77.8% and 24.6% for the DC and ACLF groups, respectively, with no deaths observed in the SC group.

3.2. Microbiota diversity, bacterial translocation, faecal calprotectin, serum bile acid, and metabolites profiles are progressively altered with increasing cirrhosis severity.

medRxiv preprint doi: https://doi.org/10.1101/2025.02.13.25322003; this version posted February 14, 2025. The copyright holder for this preprint (which was not certified by peer review) is the author/funder, who has granted medRxiv a license to display the preprint in perpetuity. All rights reserved. No reuse allowed without permission.

Initial analysis focused on the composition of the faecal microbiota, plasma bile acids, urinary metabolites and serum metabolites between cirrhosis severity groups in comparison to HCs. Faecal microbiota diversity, both the number of bacterial genera detected (**Figure 1A)** and the Inverse Simpson diversity index (**Figure 1B**), was lower in patients with more advanced cirrhosis compared to all other groups. Clustering analysis using non-metric multidimensional scaling (NMDS) shows separation in gut microbiota composition between ACLF and HC, with DC clustered between HC and ACLF, while SC clustered closely to HC (**Figure 1C; Supplementary File 2**). The overall effect of disease severity was tested using a PERMANOVA test (R2 = 13.5%; P = 0.0001) and a pairwise comparison showed that the ACLF group clustered separately ($P < 0.05$) from DC, SC, and HC groups with DC also different to the HC group (**Supplementary File 6**). To assess the associations between clinical metadata variables, NMDS analysis was specifically conducted on faecal sequencing data from patients with cirrhosis excluding HCs. Envfit analysis was used to examine the influence of 69 clinical variables on microbiota composition. Forty-one clinical variables were significantly associated with microbiota composition in patients with cirrhosis, with measures of cirrhosis severity exhibiting the most pronounced impact (**Supplementary Figure 1A; Supplementary File 7**). For the purposes of visualisation the ten clinical variables with the highest R2 values with the strongest association with the microbiota composition were overlaid on the NMDS plot and were all correlated with cirrhosis severity (**Supplementary Figure 1B; Supplementary File 7**).

NMDS plots comparing plasma bile acid composition indicated higher divergence amongst HC samples, and an increasing convergence (clustering) with cirrhosis severity (PERMANOVA: P=0.0001) (**Figure 1D; Supplementary File 3,6**). Both urine (PERMANOVA: P=0.0001) and plasma metabolites (PERMANOVA: P=0.0001) showed significant separation in clustering based on cirrhosis severity with similar NMDS clustering with tightly clustered HC samples and divergent cirrhosis patient samples, particularly for ACLF (**Figure 1E-F; Supplementary File 6**). Multivariate analysis, after obvious exclusions including for dominant glucose or ethanol peaks, for example, showed separation of the four study cohorts (HC, n=36; SC, n=8; DC, n=67; and ACLF, N=36) with pairwise multilevel comparison showing significant differences between all groups except SC and DC ($P < 0.05$). This was also

medRxiv preprint doi: https://doi.org/10.1101/2025.02.13.25322003; this version posted February 14, 2025. The copyright holder for this preprint (which was not certified by peer review) is the author/funder, who has granted medRxiv a license to display the preprint in perpetuity. All rights reserved. No reuse allowed without permission.

263 confirmed visually by the NMDS plots (**Figure E; Supplementary File 5**) and relative metabolite levels
264 per grouping for TMAO, hippurate (**Figure 3F; Supplementary File 6**) and for creatinine, citrate,
265 dimethylamine, formate and mannitol (**Supplementary Figure 3**).

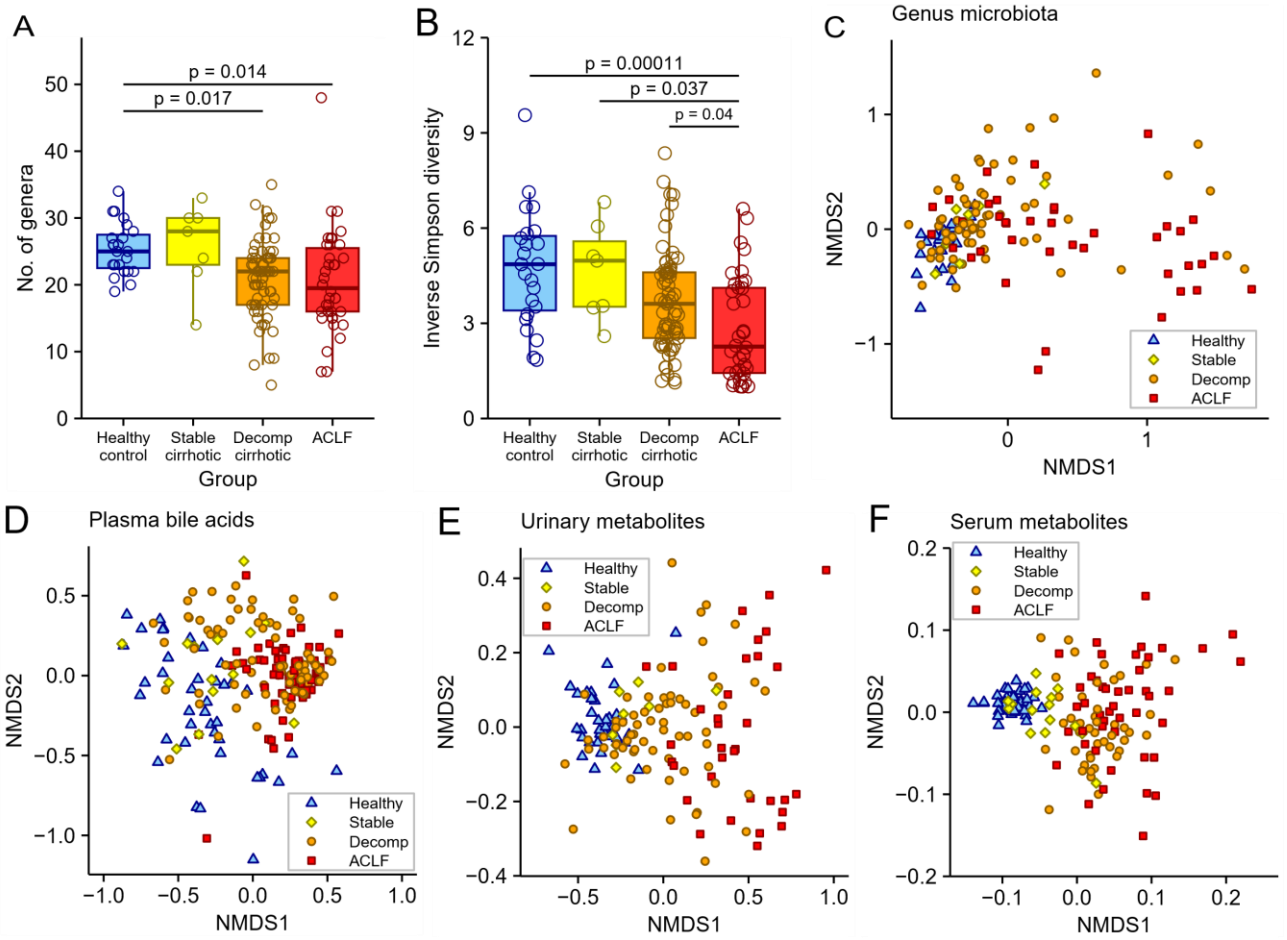

266

267 **Figure 1: Comparison of faecal microbiota diversity, plasma bile acids, and metabolites profiles in**
268 **cirrhosis and healthy controls.**

269 (A) Number of genera detected in each participant's faecal sample by cirrhosis severity and HC. (B)
270 Faecal microbiota diversity measured using the Inverse Simpson diversity index by cirrhosis severity
271 vs HC. NMDS ordination shows dissimilarity indices via Bray-Curtis distances between individual
272 participants coloured by cirrhosis severity vs HC (D) plasma bile acids (E) urinary metabolites and (F)

medRxiv preprint doi: https://doi.org/10.1101/2025.02.13.25322003; this version posted February 14, 2025. The copyright holder for this preprint (which was not certified by peer review) is the author/funder, who has granted medRxiv a license to display the preprint in perpetuity. All rights reserved. No reuse allowed without permission.

serum metabolites. Dot and box plots show median and interquartile ranges of data with circles showing each individual participant.

3.3. Genus-level microbiota composition at different cirrhosis severities reveals a progressive overabundance of *Enterococcus* with reductions in commensal taxa.

To investigate alterations in gut microbiota composition in more detail, bacterial genus profiles within individual participants were examined. Stacked bar plots showing the ten most abundant bacterial genera illustrate an increasing dominance of *Enterococcus* in more advanced cirrhosis i.e. DC and ACLF groups (**Figure 2A**). Differential abundance of bacterial genera is represented in a heat map showing significant associations between faecal bacterial genera comparing the three cirrhosis groups with HC (**Figure 2B; Supplementary file 8**). *Ruminococcus, Roseburia,* and *Lachnospira* showed the strongest negative association with cirrhosis severity with the lowest abundances in ACLF and DC patients compared to HC (**Figure 2C-E**). *Enterococcus* and *Staphylococcus* showed the strongest positive association with cirrhosis severity with highest abundance in ACLF relative to HC (**Figure 2FH**), while *Streptococcus* abundance was higher in DC and SC compared to HC (**Figure 2G)**. *Enterococcus* abundance was markedly higher in the ACLF patient group compared to HC (**Figure 2C)**. Conversely, a proportion of more severely ill patients with cirrhosis have gut microbiota dominated by *Enterococcus*, with significantly elevated levels observed in DC and ACLF. In a quarter of ACLF patients, the relative abundance of *Enterococcus* exceeded 75%.

medRxiv preprint doi: https://doi.org/10.1101/2025.02.13.25322003; this version posted February 14, 2025. The copyright holder for this preprint (which was not certified by peer review) is the author/funder, who has granted medRxiv a license to display the preprint in perpetuity.
All rights reserved. No reuse allowed without permission.

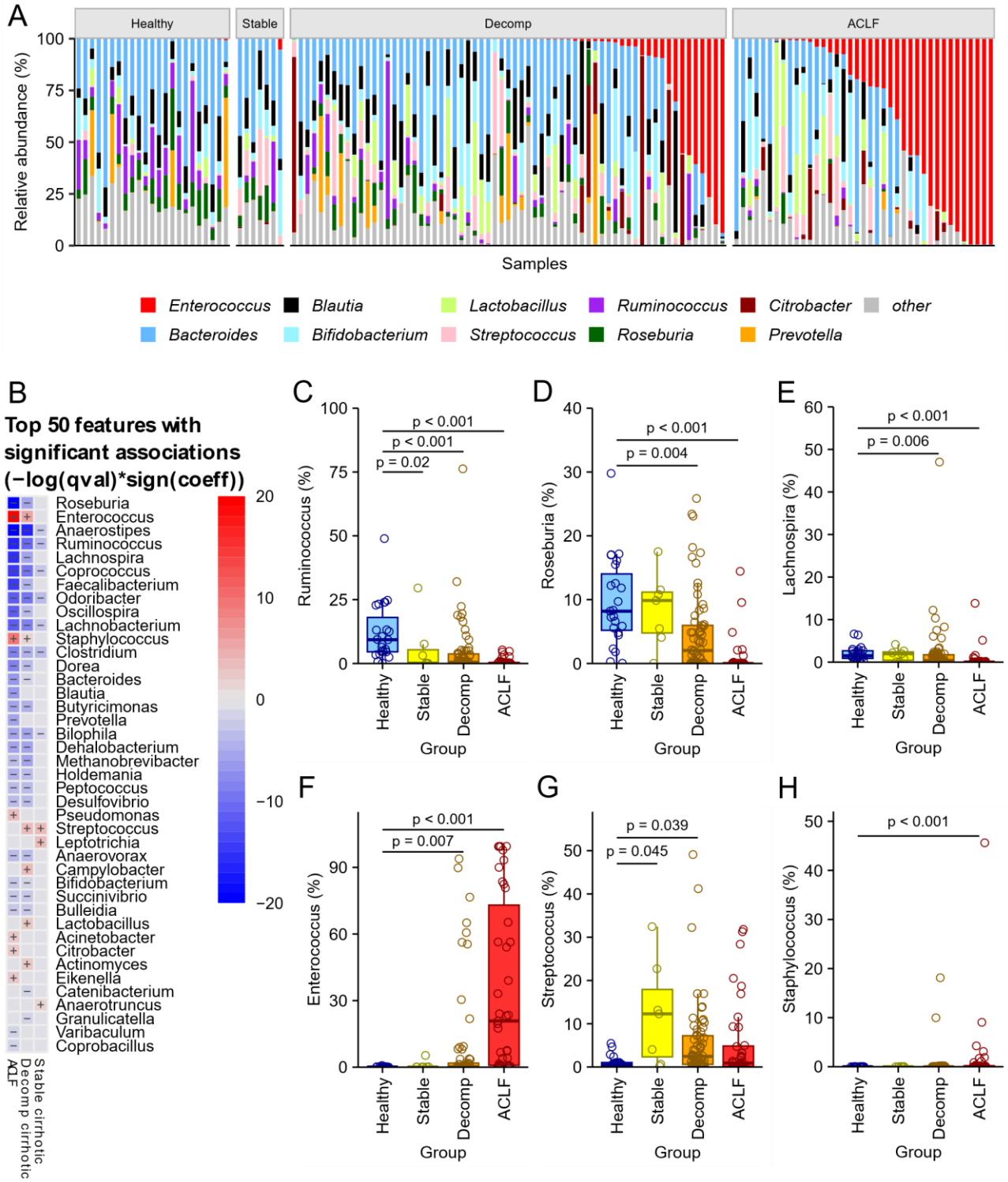

Figure 2: Microbiota genus composition in cirrhosis vs. healthy controls.

medRxiv preprint doi: https://doi.org/10.1101/2025.02.13.25322003; this version posted February 14, 2025. The copyright holder for this preprint (which was not certified by peer review) is the author/funder, who has granted medRxiv a license to display the preprint in perpetuity. All rights reserved. No reuse allowed without permission.

(A) Stacked bar plots show the ten most abundant bacterial genera in faecal samples stacked by overall abundance, and with participants ordered within cirrhosis severity categories by proportion of *Enterococcus*. (B) The heat map displays MaAslin2 analysis of significant associations between faecal genus abundance and cirrhosis severity with HC used as a reference. The three genera with the strongest negative effect size for cirrhosis severity determined by MaAslin2 using HC as a reference and shown as box and dot plots were (C) *Ruminococcus*, (D) *Roseburia*, and (E) *Lachnospira*. The three genera with the strongest positive effect size for cirrhosis severity determined by MaAsLin2 using HC as a reference and shown as box and dot plots were (F) *Enterococcus*, (G) *Streptococcus*, and (H) *Staphylococcus*. Dot and box plots show median and interquartile ranges of data with circles showing each individual participant.

3.4. Plasma bile acids and urinary metabolites correlate with specific gut microbiota taxa with increasing cirrhosis severity.

To determine the impact of cirrhosis severity on alterations in plasma bile acids, urinary metabolites, and serum metabolites, we correlated these, using MaAsLin2, with faecal bacterial genera to investigate their associations with gut microbiota composition and provide putative insights into alterations in microbiome function. The primary bile acids taurochenodeoxycholic acid (TCDCA), glycochenodeoxycholic acid (GCDCA), taurocholic acid (TCA) and glycocholic acid (GCA) were higher in the plasma of patients with cirrhosis compared to HC, while other bile acids were lower than in HC (**Figure 3A; Supplementary File 9**). TCDCA and GCDCA showed the strongest effect size with higher concentrations in all three cirrhosis cohorts relative to HC (**Figure 3B-C; Supplementary Figure 3**). Contrasting plasma bile acid concentrations with the percentage of bacterial genera showed that *Enterococcus* abundance was positively correlated with primary bile acids including TCDCA, while *Ruminococcus*, *Coprococcus*, and *Roseburia* were negatively correlated with primary bile acid concentration (**Figure 3D; Supplementary Figure 2**).

Analysis of urinary metabolites showed several metabolites differing by cirrhosis severity relative to HC (**Figure 3E; Supplementary File 10**). Two metabolites, hippurate (**Figure 3F**) and Trimethylamine

medRxiv preprint doi: https://doi.org/10.1101/2025.02.13.25322003; this version posted February 14, 2025. The copyright holder for this preprint (which was not certified by peer review) is the author/funder, who has granted medRxiv a license to display the preprint in perpetuity. All rights reserved. No reuse allowed without permission.

N-oxide (TMAO) (**Figure 3G**), were identified as products of gut microbial metabolism and both were lower in patients with cirrhosis compared to HC, and lower in ACLF than in SC or DC (**Figure 3F-G**; **Supplementary Figure 2**). Contrasting urinary metabolites with the percentage proportion of bacterial genus showed that *Enterococcus* abundance was negatively correlated with several metabolites including hippurate and TMAO, while *Ruminococcus*, *Coprococcus*, and *Roseburia* were positively correlated with hippurate and TMAO (**Figure 3H; Supplementary Figure 3**).

Similar differences were seen in plasma metabolites with significant differences between cirrhosis cohorts and HC (**Supplementary Figure 4A; Supplementary File 11**) amongst several plasma metabolites (**Supplementary Figure 4B-G**). Similarly, *Enterococcus* abundance correlated with changes in a number of plasma metabolites (**Supplementary Figure 4H**).

These findings show a pattern characterised by elevated concentrations of primary bile acids in plasma and reduced quantities of recognised microbial metabolites in the urine among cirrhosis patients with more advanced disease.

medRxiv preprint doi: https://doi.org/10.1101/2025.02.13.25322003; this version posted February 14, 2025. The copyright holder for this preprint (which was not certified by peer review) is the author/funder, who has granted medRxiv a license to display the preprint in perpetuity.
All rights reserved. No reuse allowed without permission.

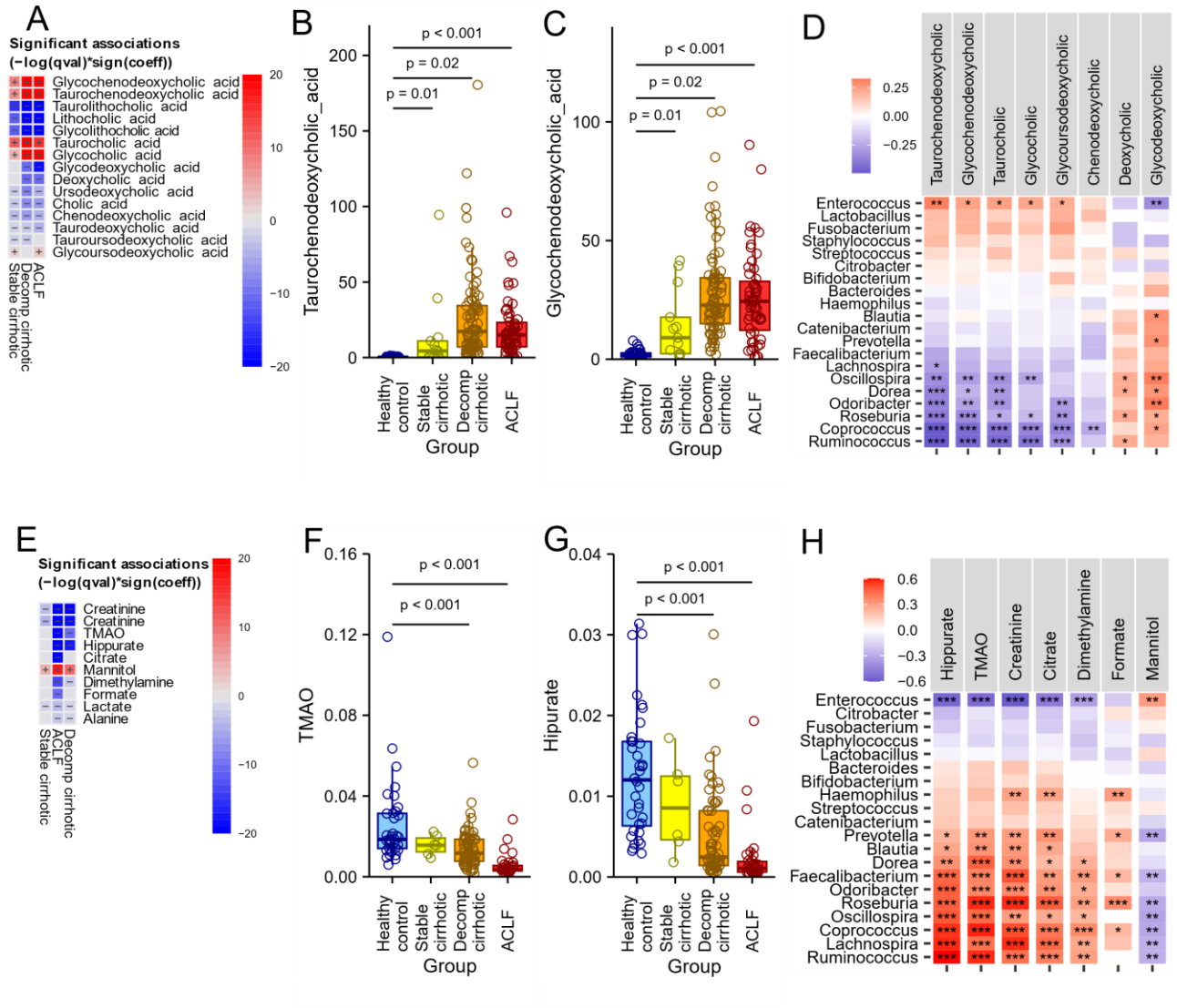

Figure 3: Plasma bile acids, urinary metabolites, and correlations with abundance of faecal bacterial genera.

(A) The heatmap displays MaAslin2 analysis results of significant associations between plasma bile acid concentrations and cirrhosis cohorts using HC as a reference. The two plasma bile acids with the strongest positive effect size for cirrhosis severity determined by MaAslin2 using HC as a reference and shown as box and dot plots were (B) Taurochenodeoxycholic acid and (C) Glycochenodeoxycholic acid. (D) Pearson correlations between the normalised relative abundance of the top twenty most

medRxiv preprint doi: https://doi.org/10.1101/2025.02.13.25322003; this version posted February 14, 2025. The copyright holder for this preprint (which was not certified by peer review) is the author/funder, who has granted medRxiv a license to display the preprint in perpetuity. All rights reserved. No reuse allowed without permission.

abundant faecal bacterial genera (comprising 98% of the microbiota) and normalised plasma bile acid concentrations showing bile acids with significant correlations. (E) The heatmap displays MaAslin2 analysis results of significant associations between urinary metabolite concentrations and cirrhosis severity using HC as a reference. The two urinary metabolites with the strongest negative effect size for cirrhosis severity determined by MaAslin2 using HC as a reference and shown as box and dot plots were (F) Trimethylamine N-oxide (TMAO) and (G) Hippurate. (H) Pearson correlations between the normalised relative abundance of the top twenty most abundant faecal bacterial genera (comprising 98% of the microbiota) and normalised urinary metabolite concentrations showing metabolites with significant ($P < 0.05$) correlations. Full correlations shown in Supplementary Figure 3 and 4.

3.5. Clinical variables link to overall microbiota profiles, with further associations in advanced cirrhosis of *Enterococcus* with antibiotic usage and resistance profiles

Next, we carried out an exploratory analysis to determine how clinical parameters might be associated with gut microbiota composition, using the envfit function, focusing on each clinical variable and overall microbiota beta-diversity. The ten clinical variables with the strongest association with faecal microbiota composition were plotted overlaying an NMDS plot (**Supplementary Figure 1).** Several clinical factors correlated with microbiota composition, with conventional measures of cirrhosis severity showing the strongest association (**Supplementary Figure 1, Supplementary File 7**). Composite clinical scores are used to classify cirrhosis severity and for prognostication. Of those included in this analysis, ACLF grade, MELD score, Child-Pugh grade and score, and UKELD score were all associated with microbiota composition, in keeping with the study phenotyping of the cirrhosis cohorts, i.e. SC, DC, and ACLF.

Antibiotic use, oral food intake, and lactulose use were clinical variables identified as both having an association with microbiota composition, and considered likely to have a direct influence on the gut microbiota **(Supplementary File 2)**. Differential abundance testing was carried out using MaAslin2 for antibiotic use, oral food intake, and lactulose use along with cirrhosis severity was included within the MaAslin2 model to adjust for covariance (**Supplementary File 12**). Antibiotic use, oral food intake,

medRxiv preprint doi: https://doi.org/10.1101/2025.02.13.25322003; this version posted February 14, 2025. The copyright holder for this preprint (which was not certified by peer review) is the author/funder, who has granted medRxiv a license to display the preprint in perpetuity. All rights reserved. No reuse allowed without permission.

lactulose use, all showed significant effects on differential abundance of genus within the patient cohort when adjusted for covariance. Comparing the genus with the large difference in abundance in cirrhosis patients receiving or not receiving enteral intake, *Roseburia* abundance was lower in patients not receiving nutrition *via* enteral routes (normal oral intake and by enteral tube feeding), while *Enterococcus* abundance was higher (**Figure 4A**). Similarly, *Roseburia* abundance was lower in patients receiving antibiotics, while *Enterococcus* abundance was higher (**Figure 4B**). Results were unchanged when excluding the 5 patients only receiving rifaximin as antibiotic treatment. Lactulose use was associated with a higher relative abundance of *Bifidobacterium* within the patient cohort between those receiving lactulose and those not (Figure 4E). *Enterococcus* remained significantly higher abundance in DC and ACLF severity groups compared to HC when adjusted for antibiotic use, oral food intake indicating an independent effect of all three factors on *Enterococcus* abundance (**Supplementary Table 2**).

The cirrhosis group as a whole received a total of 19 different types of antibiotics (**Figure 4F; Supplementary Table 2.** The most frequently used antibiotics were piperacillin/tazobactam (Tazocin) (33 patients) and 16 Meropenem (16 patients) totalling 37% of patients while 48 (36%) received no antibiotics. The remaining 17 antibiotics were given to 6 or fewer patients with 8 antibiotics only given to one patient. To visualise the complexities of this antibiotic administration, data was visualised as a heatmap with patients clustered by antibiotic use and antibiotics clustered by co-occurrence (**Figure 4C**). Associations of gut bacterial genus differential abundance with all individual antibiotic administration was tested in a MaAslin2 model with only piperacillin/tazobactam (Tazocin) and meropenem individually associated with abundance of *Enterococcus* (**Supplementary Table 8 Figure 4C**). Five out of 48 patients not currently receiving antibiotics also showed higher *Enterococcus* relative abundance (**Figure 4C**). This cirrhosis cohort included a range of aetiologies, however, cause of cirrhosis did not significantly associate with gut microbiota composition. Rather, cirrhosis severity, antibiotics, and nutritional intake use was the primary factor that co-associated with a dominant *Enterococcus* gut microbiota signature in patients with most severe disease i.e. DC and ACLF (**Supplementary figure 7AB**).

medRxiv preprint doi: https://doi.org/10.1101/2025.02.13.25322003; this version posted February 14, 2025. The copyright holder for this preprint (which was not certified by peer review) is the author/funder, who has granted medRxiv a license to display the preprint in perpetuity. All rights reserved. No reuse allowed without permission.

To probe *Enterococcus* traits in more detail, five isolates obtained from five different patient faecal samples (one sample from the DC cohort and four from the ACLF cohort) underwent whole genome sequencing and were identified as *Enterococcus faecium*. Comparing the similarities of these 5 novel isolates with an additional publicly available 185 *E. faecium* genomes (retrieved from the NCBI GenBank database) using midpoint rooted maximum-likelihood tree showed a diversity of *E. faecium* genomes with no single clonal group colonising patients with cirrhosis indicating that the *E. faecium* isolates did not originate from the same source (**Figure 4D**). The five *E. faecium* cirrhosis isolate genomes were aligned against virulence-related gene profiles, antibiotic resistance genes, and bile resistance genes (**Figure 4E**). These isolates contained between 12 and 17 of the 20 antibiotic resistance genes analysed (**Figure 4E**); 5 genes encoding aminoglycoside resistance, 7 *van* genes encoding vancomycin resistance, 3 encoding macrolides resistance, 2 encoding tetracycline resistance, and 2 trimethoprim resistance. The two bile acid resistance genes *bsh* and *gltK* were present in all patient isolates, and in the genomes of 95% of all 190 isolates from public databases (**Figure 4F**).

Taken together, these data indicate that clinical factors such as reduced enteral nutritional intake and exposure to the broad-spectrum beta-lactam antibiotics piperacillin/tazobactam (Tazocin) and meropenem were strongly linked to higher levels of *Enterococcus* and decreased abundance of commensal genera in patients with cirrhosis. Broad-spectrum beta-lactam antibiotics are commonly administered to DC and ACLF patients as part of their treatment regimen. *Enterococcus* isolates obtained and sequenced from these patients were identified as *E. faecium* and were found to encode various antibiotic and bile acid resistance genes, indicating potential bacterial survival mechanisms and pathogenicity.

medRxiv preprint doi: https://doi.org/10.1101/2025.02.13.25322003; this version posted February 14, 2025. The copyright holder for this preprint (which was not certified by peer review) is the author/funder, who has granted medRxiv a license to display the preprint in perpetuity.
All rights reserved. No reuse allowed without permission.

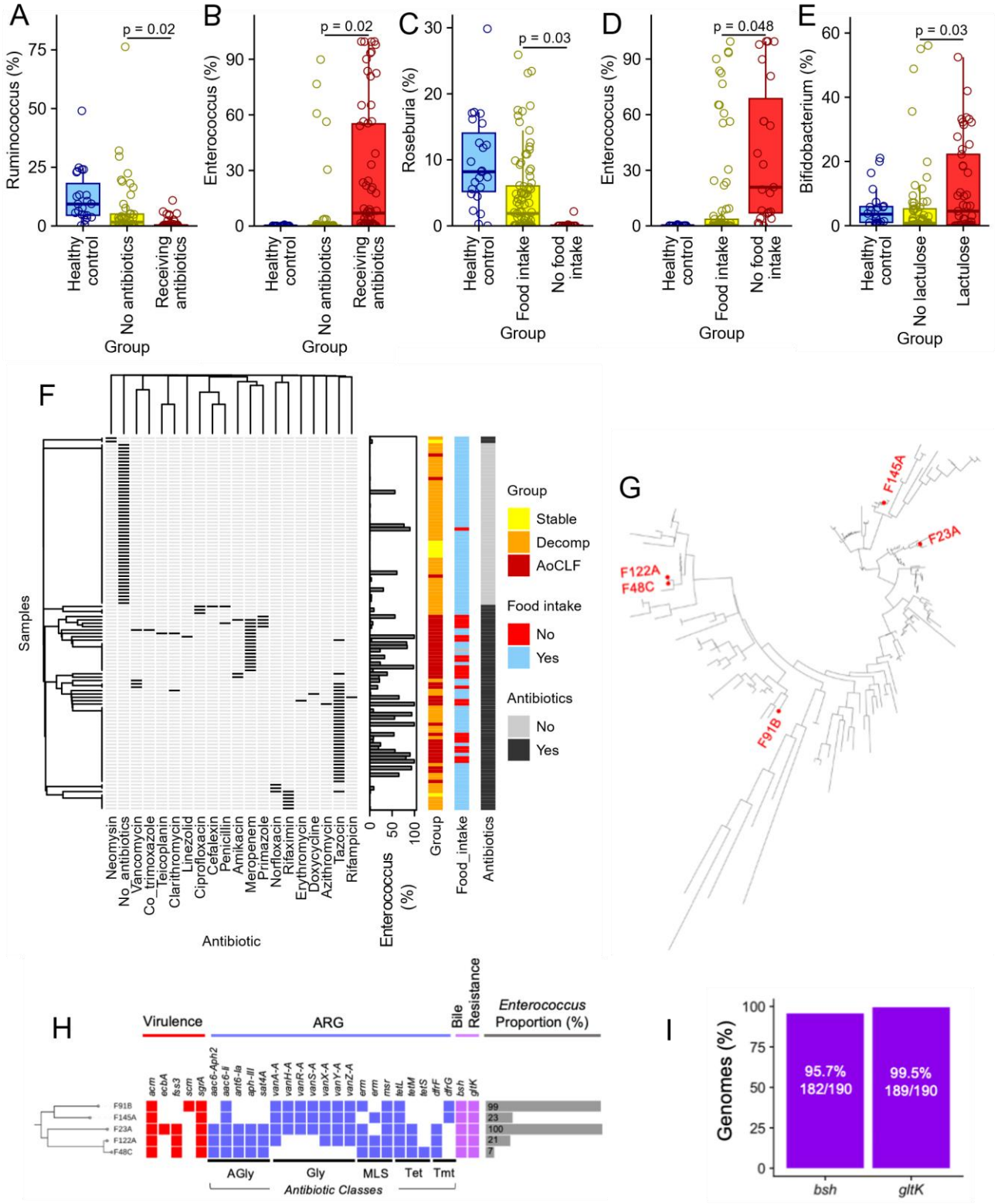

419

medRxiv preprint doi: https://doi.org/10.1101/2025.02.13.25322003; this version posted February 14, 2025. The copyright holder for this preprint (which was not certified by peer review) is the author/funder, who has granted medRxiv a license to display the preprint in perpetuity. All rights reserved. No reuse allowed without permission.

Figure 4: Oral food intake, receiving antibiotics, and *Enterococcus faecium* genomic data.

The differentially abundant genera with the strongest negative and positive effect sizes for antibiotics with patients not receiving antibiotics as the reference were (A) *Ruminococcus* and (B) *Enterococcus*. The differentially abundant genera with the strongest negative and positive effect sizes for nutritional intake with patients not receiving enteral as the reference were (C) *Roseburia* and (D) *Enterococcus*. The differentially abundant genera with the strongest positive effect size for lactulose use with patients not receiving lactulose as the reference was (E) *Bifidobacterium*. (F) Clustered individual antibiotics received by patients with cirrhosis cohort, nutritional status, and relative abundance of *Enterococcus* in each sample. (G) A midpoint rooted maximum-likelihood tree consisted of 190 *Enterococcus faecium* genomes, including 5 novel *E. faecium* isolates obtained from cirrhosis patients, as highlighted in the tree. (H) Novel *E. faecium* genomes (n=5) from cirrhosis patients aligned with virulence-related gene profiles, virulence (using VFDB), ARG (Antibiotic Resistance Genes; using ARG-ANNOT) and bile resistance genes (*bsh* and *gltK*), accordingly. Proportion of *Enterococcus* (genus level; based on 16S rRNA sequence data) in the corresponding faecal samples was also indicated in the horizontal bar chart. (I) Proportion of detectable bile resistance genes (%) *bsh* and *gltK* in 190 *E. faecium* genomes, suggesting that these two genes belong to the core genome of *E. faecium*.

3.6. Faecal microbiota and markers of bacterial translocation, intestinal and systemic inflammation, and monocyte exhaustion.

To explore links between gut barrier dysfunction and translocation of intestinal bacteria and/or their products from the gut into the systemic circulation, we determined the number of copies of 16S rDNA in whole blood from cirrhosis patients and HC. The number of copies of 16S rDNA in the blood was lowest in HC in keeping with a degree of 'physiological translocation' and displayed a stepwise increase with severity of cirrhosis (**Figure 5A**). To identify associations with the faecal microbiota, we correlated copies of 16S rDNA in the blood against percentages of bacterial genera (**Figure 5B**), with *Enterococcus* most strongly positively correlated (**Figure 5C**), and *Lachnospira* most negatively

medRxiv preprint doi: https://doi.org/10.1101/2025.02.13.25322003; this version posted February 14, 2025. The copyright holder for this preprint (which was not certified by peer review) is the author/funder, who has granted medRxiv a license to display the preprint in perpetuity. All rights reserved. No reuse allowed without permission.

446 correlated (**Figure 5C**). Faecal calprotectin as a conventional marker of non-specific gut mucosal
447 inflammation also showed a stepwise increase with cirrhosis severity compared to HC (**Figure 5D**).
448 Faecal calprotectin was positively correlated with relative abundance of *Enterococcus* **(Figure 5E**) and
449 negatively correlated with *Lachnospira* (**Figure 5E**).

450 The innate immune function of CD14+ monocytes isolated from peripheral blood obtained from
451 cirrhosis patients and HCs was assessed by stimulation with TLR 2/4/9 agonists *in vitro*, with
452 unstimulated controls, and the percentage of Tumour necrosis factor-alpha (TNF- α), Interleukin-6
453 (IL-6), and monocyte human leukocyte antigen-DR (HLA-DR) positive monocytes identified by flow
454 cytometry. Monocytes from DC and ACLF patients showed attenuated proinflammatory responses
455 (TNF-α and IL-6) to Pam3, LPS and CpG challenge, indicating reduced innate responses to pathogen-
456 induced TLR signalling pathways. (**Supplementary Figure 1**). To identify cirrhosis-associated
457 alterations in monocyte function and associations with factors linked to the microbiota, the
458 percentage of TNF-a or IL-6 positive monocytes were correlated with copies of 16S rDNA in whole
459 blood, faecal calprotectin, and the twenty faecal genera with the highest overall abundance (**Figure**
460 **5I; Supplementary Figure 6**). The number of copies of bacterial DNA in whole blood positively
461 correlated with the percentage of IL-6 positive unstimulated monocytes, while the number of genera
462 positively correlated with the percentage of TNF-alpha and IL-6 positive LPS-stimulated monocytes
463 (**Figure 5I**). *Lachnospira* showed positive associations and *Enterococcus* negative associations with
464 the percentage of TNF-alpha and IL-6 positive LPS stimulated monocytes (**Figure 5J**) and *Enterococcus*
465 with TNF-alpha positive Pam3 stimulated monocytes (**Figure 5IK**).

466 These findings reveal contrasting associations between *Enterococcus* and other commensal bacterial
467 genera, such as *Lachnospira*, on markers of intestinal permeability, intestinal and systemic
468 inflammation, and monocyte innate immune function.

469

470

medRxiv preprint doi: https://doi.org/10.1101/2025.02.13.25322003; this version posted February 14, 2025. The copyright holder for this preprint (which was not certified by peer review) is the author/funder, who has granted medRxiv a license to display the preprint in perpetuity.
All rights reserved. No reuse allowed without permission.

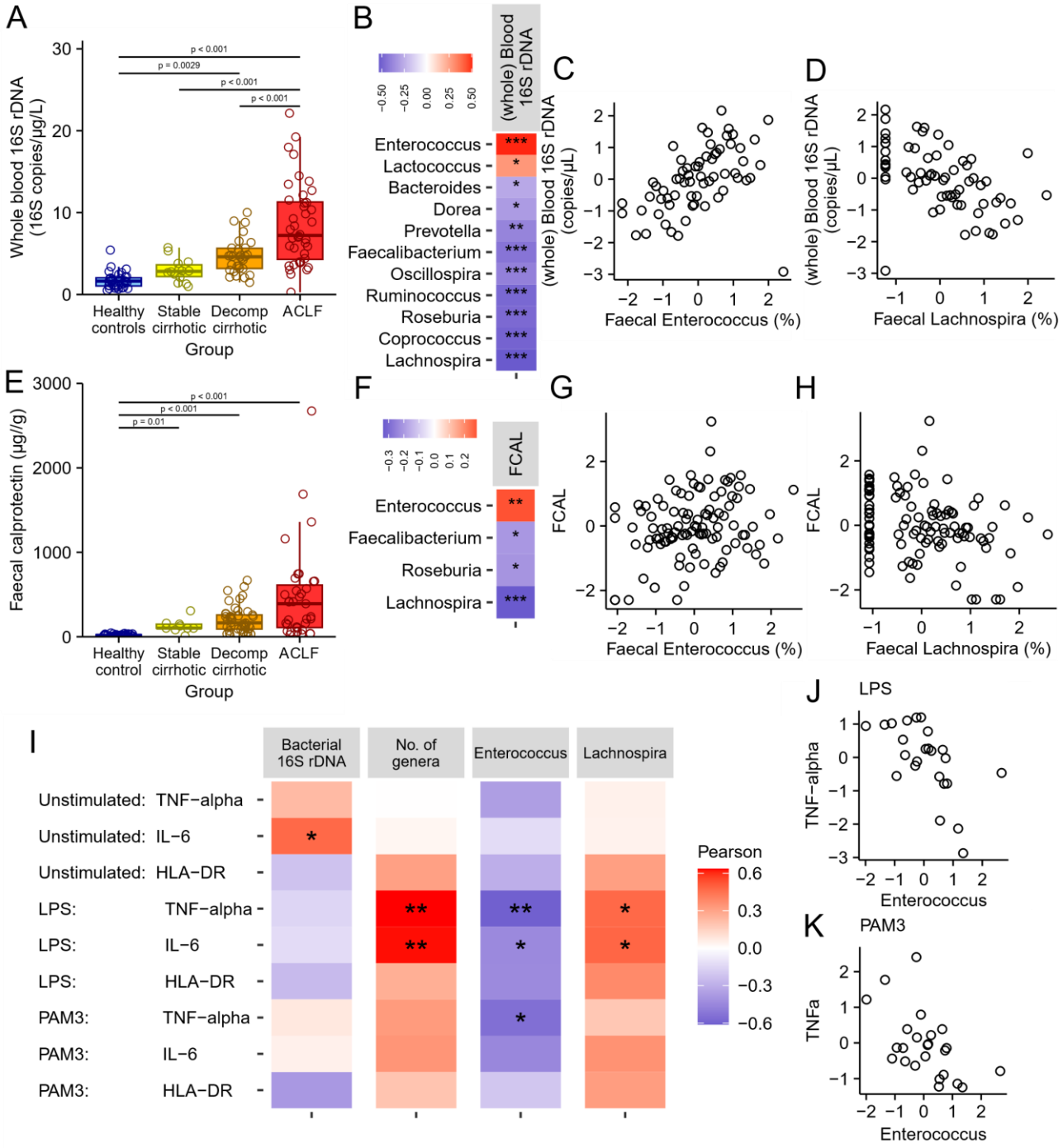

471

472 **Figure 5. Markers of intestinal permeability and intestinal inflammation and correlations of**
473 **stimulated monocyte activation with (whole) blood 16S rDNA and faecal microbiota.**

medRxiv preprint doi: https://doi.org/10.1101/2025.02.13.25322003; this version posted February 14, 2025. The copyright holder for this preprint (which was not certified by peer review) is the author/funder, who has granted medRxiv a license to display the preprint in perpetuity. All rights reserved. No reuse allowed without permission.

(A) Copies of 16S rDNA in participant blood by cirrhosis severity vs HC. (B) Significant correlations between copies of 16S rDNA in participant blood and percentage of genera in the faecal microbiota. (C) Scatter plot of copies of 16S rDNA in blood against faecal *Enterococcus* for each participant. (D) Scatter plot of copies of 16S rDNA in blood against faecal *Lachnospira* for each participant. (E) Faecal calprotectin concentration by cirrhosis severity vs HC. (F) Significant correlations between faecal calprotectin concentration and percentage of genera in the faecal microbiota. (G) Scatter plot of faecal calprotectin concentration against faecal *Enterococcus* percentage for each participant. (H) Scatter plot of faecal calprotectin concentration against faecal *Lachnospira* percentage for each participant. (I) Percentage of monocytes showing TNF-α and IL-6 production and HLA-DR expression in response to antigen stimuli (LPS/TLR-4; Pam3CSK4/TLR-2, CpG/TLR-9) correlated separately with whole blood 16S rDNA, number of faecal genera, faecal *Enterococcus* percentage and faecal *Lachnospira* percentage. Stars (*) indicate statistical significance ($P < 0.05$) after adjustment for multiple testing. (J) Scatter plot of percentage of TNF-alpha positive LPS stimulated monocytes against faecal *Enterococcus* percentage for each participant. (K) Scatter plot of percentage of TNF-alpha positive PAM3 stimulated monocytes against faecal *Enterococcus* percentage for each participant.

medRxiv preprint doi: https://doi.org/10.1101/2025.02.13.25322003; this version posted February 14, 2025. The copyright holder for this preprint (which was not certified by peer review) is the author/funder, who has granted medRxiv a license to display the preprint in perpetuity. All rights reserved. No reuse allowed without permission.

4. Discussion

We found higher relative abundance of *Enterococcus* in the gut microbiota of patients with cirrhosis, particularly in those with advanced disease and receiving broad spectrum antibiotics, accompanied by a lower abundance of obligate anaerobic commensal genera. This shift is consistent with patterns seen in other conditions with compromised intestinal barrier function, such as preterm infants (Hufnagel et al., 2007) and Graft-versus-Host Disease (Garrett, 2020), as well as other studies in ACLF (Lee et al., 2024a, 2024b; Solé et al., 2021). These findings suggest that *Enterococcus*, an opportunistic pathogen, may exploit disrupted gut microbial communities and diminished colonisation resistance to thrive, especially in advanced disease states with multiple gut microbiota modulating treatments.

Multiple factors may contribute to the selection and proliferation of resident *Enterococcus* strains in the gut of cirrhosis patients. Antibiotic use is one such factor, as many of the patients with high *Enterococcus* levels had received broad-spectrum beta-lactam antibiotics like Piperacillin/tazobactam or meropenem. These antibiotics are commonly administered to hospitalised DC and ACLF patients for treating suspected infections, often before culture results are available, and *Enterococcus* exhibits intrinsic resistance to beta-lactam antibiotics (Zapun et al., 2008), potentially providing a selective advantage. Additionally, the *E. faecium* isolates in this study encoded genes conferring bile acid resistance (Zhang et al., 2013), which may further facilitate persistence in the bile-rich environment characteristic of advanced cirrhosis (Kakiyama et al., 2013). Elevated intestinal luminal bile acids in cirrhosis, particularly primary bile acids, can alter the gut microbial environment (Ridlon et al., 2013), often reducing bile-sensitive commensals like *Roseburia* and providing an ideal niche for *Enterococcus* to overgrow.

This relative overgrowth of *Enterococcus* in the gut microbiota, especially strains with virulence genes like *acm* and *sgrA* (encoded in all strains isolated from this study cohort), which enhance adhesion and translocation, presents significant clinical implications. These strains may be associated with systemic infections that can exacerbate cirrhosis-related complications, such as progression from a

medRxiv preprint doi: https://doi.org/10.1101/2025.02.13.25322003; this version posted February 14, 2025. The copyright holder for this preprint (which was not certified by peer review) is the author/funder, who has granted medRxiv a license to display the preprint in perpetuity. All rights reserved. No reuse allowed without permission.

stable state to DC and ACLF (Hendrickx et al., 2009; Nallapareddy et al., 2008). Moreover, bacterial sepsis is a significant complication in patients with cirrhosis, an increasing recognition of the threat of antimicrobial resistance (Piano et al., 2019; Wong et al., 2021). Carriage of multidrug resistant strains (as indicated by our genomic analysis) may contribute to greater clinical complication episodes by way of hepatic decompensation, organ failure and mortality rates, due to increased translocation of *Enterococcus* via a dysfunctional and inflamed gut barrier into the bloodstream. Furthermore, as *Enterococcus* appears to dominate more severely ill patients to the exclusion of other potential pathogens, this pattern raises questions about its source. Genomic analysis showed divergent strains of *E. faecium* were present in patients rather than any common clonal lineages, which would be the case if multiple patients had acquired the *E. faecium* from each other or from the same hospital environment. This indicated that the *E. faecium* are more likely to represent resident gut strains already in the patient rather than nosocomial infections. Further investigation involving a larger number of isolates will be valuable to confirm these findings.

As faecal *Enterococcus* abundance increased, we observed a corresponding significant decline in key commensal bacterial genera including *Roseburia*, *Ruminococcus*, *Coprococcus*, and *Faecalibacterium*, with many ACLF patients showing an almost complete relative absence. These genera are essential for SCFA production, such as butyrate (Flint et al., 2012), which supports intestinal barrier integrity. The loss of these beneficial microbes is a common feature in cirrhosis (Acharya and Bajaj, 2019) that is linked to the development of gut barrier failure, pathological microbial translocation and cirrhosis-associated immune dysfunction. Their decline appears to be further exacerbated by common therapeutic factors in the treatment of advanced cirrhosis, such as the use of broad-spectrum antibiotics, which impact antibiotic-sensitive species (Zimmermann and Curtis, 2019), and a reliance on fibre-deficient diets, particularly among patients dependent on enteral or parenteral nutrition (present in 45% of the ACLF group). These diets lack the necessary fermentable dietary fibre to sustain SCFA-producing microbes, worsening microbial disruption and potentially contributing to gut permeability.

medRxiv preprint doi: https://doi.org/10.1101/2025.02.13.25322003; this version posted February 14, 2025. The copyright holder for this preprint (which was not certified by peer review) is the author/funder, who has granted medRxiv a license to display the preprint in perpetuity. All rights reserved. No reuse allowed without permission.

544 This microbiota disruption is mirrored by lower urinary levels of metabolites like hippurate which is
545 a products of beneficial microbial metabolism and fibre-rich diets (Lees et al., 2013) and TMAO, which
546 is a microbial byproduct or metabolising nutrients including choline, betaine, and carnitine found in
547 meat, eggs, and fish (Pallister et al., 2017). Hippurate production, often associated with microbial
548 metabolism of phenolic compounds in fruits and vegetables, was positively correlated with
549 *Ruminococcus*, further linking microbial loss with decreased metabolic activity. Similarly, TMAO -
550 produced via hepatic conversion of trimethylamine (TMA), itself a microbial metabolite from dietary
551 sources like carnitine and lecithin - was also reduced, indicating either a reduction in dietary
552 substrates or a loss of the bacteria producing TMA or potentially a loss of liver function to convert
553 TMA into TMAO (van den Berg et al., 2023). Reduced *Ruminococcus* abundance correlated with
554 decreased urinary TMAO, reflecting not only microbial shifts but also dietary limitations and potential
555 hepatic enzymatic changes (FMO1 and FMO3) seen in advanced cirrhosis (Organ et al., 2020)
556 (Gatarek and Kaluzna-Czaplinska, 2021; Williams et al., 2010). These data suggest that microbial and
557 dietary disturbances may jointly contribute to the metabolic and immune challenges observed in
558 cirrhosis progression.

559 Further, we noted that patients with cirrhosis exhibited elevated plasma bile acids, especially
560 glycochenodeoxycholic and TCDCA, which correlated with cirrhosis severity. This increase likely
561 stems from impaired hepatic bile acid uptake and reduced conversion to secondary bile acids due to
562 the loss of deconjugating genera like *Lachnospiraceae* and *Ruminococcaceae* genera that were
563 significantly depleted in this cirrhosis cohort (Vital et al., 2019). This impaired conversion could
564 further favour the persistence of *Enterococcus*, as elevated primary bile acids can disrupt the gut
565 microbial ecosystem and inhibit commensal bacteria.

566 Consistent with microbial translocation in cirrhosis, we observed elevated copies of 16S rDNA in the
567 systemic circulation of patients, correlating with cirrhosis severity and reflecting gut barrier
568 dysfunction (Albillos et al., 2022). This microbial translocation, along with elevated faecal calprotectin
569 concentrations, and associated breakdown of gut barrier function and integrity in cirrhosis (Riva et
570 al., 2020), linking with loss of key butyrate-producing microbes like *Ruminococcus* and

medRxiv preprint doi: https://doi.org/10.1101/2025.02.13.25322003; this version posted February 14, 2025. The copyright holder for this preprint (which was not certified by peer review) is the author/funder, who has granted medRxiv a license to display the preprint in perpetuity. All rights reserved. No reuse allowed without permission.

571 *Faecalibacterium* genera in DC and ACLF patients (Fagan et al., 2015) (Bach Knudsen et al., 2018).
572 Reduced faecal short-chain fatty acids have been previously reported (Jin et al., 2019; Wang et al.,
573 2023), and a reduced capacity to ferment dietary fibre in cirrhosis patients compared to healthy
574 controls (Jin et al., 2019). *Enterococcus*, which correlated strongly with 16S rDNA copies in the blood,
575 and gut inflammation markers like faecal calprotectin, indicates its likely role in gut inflammation and
576 immune activation in these patients. In cirrhosis, the progressive loss of intestinal barrier integrity
577 allows MAMPs, and viable bacteria, like *Enterococcus*, to translocate into the bloodstream, triggering
578 systemic inflammation and further impairing immune function (Tilg et al., 2022). Indeed, previous
579 work in mice indicates that *E. faecium* triggers colonic cytokine expression, which appears to be strain
580 dependent (Seishima et al., 2019) and related to elevated faecal cytokine levels and other markers
581 of gut barrier dysfunction in DC patients (Riva et al., 2020). Conversely, *Lachnospira* were markedly
582 reduced in cirrhosis patients (Abdugheni et al., 2022), potentially resulting in the loss of the
583 protective role of SCFAs that dampen mucosal immune activation such as through activation and
584 maturation of T regulatory cells (Y et al., 2013). Coupled with impaired immune responses to
585 pathogen-associated TLR signalling, as observed in the CD14+ monocytes of cirrhotic patients, this
586 suggests a vicious cycle of gut perturbations, immune dysfunction, and bacterial translocation that
587 exacerbates systemic inflammation.

588 Interestingly, despite the widespread antibiotic use in the DC and ACLF patients, *Bifidobacterium*
589 persisted in the microbiota of patients with cirrhosis. This genus is typically considered sensitive to
590 antibiotic use (Moubareck et al., 2005), so its resilience here may be due to the frequent use of
591 lactulose, a non-absorbable disaccharide laxative often prescribed to prevent or treat hepatic
592 encephalopathy. Lactulose acts as a prebiotic, providing a substrate that *Bifidobacterium* can
593 metabolise, thereby promoting its growth. Recent studies have shown lactulose can elevate
594 *Bifidobacterium* levels in cirrhosis patients, which inhibited the antibiotic-resistant pathobiont
595 vancomycin-resistant *E. faecium* through potential mechanisms including lowering the luminal pH
596 and via acetate production (Odenwald et al., 2023). Our results add to these recent findings that

medRxiv preprint doi: https://doi.org/10.1101/2025.02.13.25322003; this version posted February 14, 2025. The copyright holder for this preprint (which was not certified by peer review) is the author/funder, who has granted medRxiv a license to display the preprint in perpetuity. All rights reserved. No reuse allowed without permission.

lactulose supplementation could help support *Bifidobacterium* populations in patients with cirrhosis (Odenwald et al., 2023).

From a therapeutic perspective, restoring the gut microbiota toward a healthier balance, or "eubiosis", could mitigate the cycle of immune dysfunction and prevent cirrhosis-related complications (Tranah et al., 2021). Dietary or microbial interventions, such as prebiotics, probiotics, or microbiome-targeted treatments, could offer a promising approach. While faecal microbiota transplantation is currently being trialled (e.g. ClinicalTrials.gov: NCT02862249, NCT06461208, NCT04932577), it carries risks for patients with advanced cirrhosis, where highly personalised or targeted microbiome interventions may be safer (Cibulková et al., 2021) and use of Cefepime to protect anaerobes in gut vs Pip Taz / meropenem. Probiotics or prebiotics aimed at restoring beneficial taxa lost in cirrhosis, such as *Roseburia*, could help inhibit *Enterococcus* overgrowth, reinforce intestinal barrier integrity, and reduce inflammation. However, these approaches are not available yet clinically or commercially, and significant investment and development is needed to bring such novel, next-generation microbiome-modulating therapies to benefit this patient population. This highlights the urgency for better antimicrobial stewardship and the development of rapid diagnostics that can better target potential pathogens while reducing the use of broad spectrum antibiotics and deescalating to avoid prolonged courses of exposure.

Our findings raise the possibility that the overgrowth of *Enterococcus* and loss of commensal microbiota may not merely correlate with disease severity, and associated conventional therapies such as the use of antibiotics and absence of a dietary fibre may also contribute to disease progression. However, our cross-sectional study design and single time-point sampling limit our ability to infer causality. Longitudinal studies, combined with animal models, could further clarify whether *Enterococcus* contributes to pathological processes in cirrhosis or is an opportunistic response to the disrupted gut environment. Additionally, refined antibiotic strategies, possibly reducing the selective pressure for *Enterococcus*, alongside targeted dietary support to foster beneficial microbes, may represent viable options to improve outcomes for these high-risk patients.

medRxiv preprint doi: https://doi.org/10.1101/2025.02.13.25322003; this version posted February 14, 2025. The copyright holder for this preprint (which was not certified by peer review) is the author/funder, who has granted medRxiv a license to display the preprint in perpetuity. All rights reserved. No reuse allowed without permission.

7. Acknowledgements

We are grateful to all the patient participants and healthy volunteers for agreeing to take part in this study, and to the clinical and liver research teams at King's College Hospital for facilitating recruitment, collecting metadata and biological sample collection. We thank the King's College Hospital Charity and a generous donation from a Liver Service User, and the Foundation for Liver Research for funding. Sequencing analysis was supported in part by the NBI Research Computing through the provision of a High Performance Computing. The authors thank the Centre for Biomolecular Spectroscopy funded by the Wellcome Trust and British Heart Foundation (ref. 202767/Z/16/Z and IG/16/2/32273).

Supplementary methods

Study participants & biological sampling

Patient participants were stratified and phenotyped according to clinically relevant groups based on the severity and time course of their underlying cirrhosis, degree of hepatic decompensation, and presence and extent of hepatic and extra-hepatic organ failure at the time of sampling. These groups were stable cirrhosis (SC; n=15), decompensated cirrhosis (DC; n=55) and acute-on-chronic liver failure (ACLF; n=57), with a separately recruited healthy control cohort (HC; n=40). SC was defined as having Child Pugh A grade(score) of A(5-6). DC was defined by the acute development of 1 or more major complications of cirrhosis, including ascites, HE, variceal haemorrhage, and bacterial infection. ACLF was defined and graded according to the number of organ failures in concordance with criteria reported in the CANONIC study (Arroyo et al., 2015; Moreau et al., 2013). Main exclusion criteria included pregnancy, hepatic or non-hepatic malignancy (HCC within Milan criteria were included), pre-existing immunosuppressive states, replicating HBV/HCV/HIV infection, and known inflammatory bowel disease. Further details are provided in the Supplementary section.

medRxiv preprint doi: https://doi.org/10.1101/2025.02.13.25322003; this version posted February 14, 2025. The copyright holder for this preprint (which was not certified by peer review) is the author/funder, who has granted medRxiv a license to display the preprint in perpetuity. All rights reserved. No reuse allowed without permission.

Patients were consecutively recruited at King's College Hospital after admission to the ward or when reviewed in the hepatology out-patient clinic, through an observational study and a clinical trial. The observational study was granted approval by the NHS Health Research Authority NRES Committee London Westminster [REC reference: 12/LO/1417] and local sponsor Research and Development department (KCH12-126). Ethical approval for the interventional trial was obtained from NHS Health Research Authority NRES Committee South Central-Oxford C (Bristol) [REC reference: 14/SC/0088] and from the Medicines and Healthcare products Regulatory Agency for Clinical Trial Authorisation [EudraCT number: 2013-004708-20; ClinicalTrials.gov NCT02019784]. The studies were conducted in compliance with the principles of the Declaration of Helsinki (1996), principles of Good Clinical Practice, Research Governance Framework and where relevant, the Medicines for Human Use (Clinical Trial) Regulations. Clinical service users and caregivers were fully consulted and involved in the design of both the study and the trial, and were given opportunities to review and feedback on overall set-up, delivery and practical aspects, including input into development of all participant facing documents. Only baseline pre-intervention data from the clinical trial participants are used in this manuscript. Fully informed consent was obtained from all participants. Some participants eligible for this study were unable to provide informed consent due to cognitive impairment arising from HE and permission from a legal representative was sought.

Patient participants, or their legal representative in the case of incapacitation of a potential participant, provided written informed consent within 48 hours of presentation. Patients were managed according to standard evidence-based protocols and guidelines (European Association for the Study of the Liver., 2018). Patient and Public Involvement and Engagement was undertaken with a patient advisory group to determine acceptability of the studies, provided their perspective on study design, informational material, measures to minimise participation burden and agreeing on a dissemination plan of the findings.

Patient participants were stratified into and phenotyped according to clinically relevant groups based on the severity and time course of their underlying cirrhosis, degree of stability and hepatic decompensation, and presence and extent of hepatic and extra-hepatic organ failure at the time of

medRxiv preprint doi: https://doi.org/10.1101/2025.02.13.25322003; this version posted February 14, 2025. The copyright holder for this preprint (which was not certified by peer review) is the author/funder, who has granted medRxiv a license to display the preprint in perpetuity. All rights reserved. No reuse allowed without permission.

674 sampling. These groups were stable cirrhosis, acutely decompensated cirrhosis (AD) and acute-on-
675 chronic liver failure (ACLF), with a separately recruited healthy participant control cohort. AD was
676 defined by the acute development of 1 or more major complications of cirrhosis, including ascites,
677 hepatic encephalopathy, variceal haemorrhage, and bacterial infection. ACLF was defined and graded
678 according to the number of organ failures in concordance with criteria reported in the CANONIC study
679 (Arroyo et al., 2016; Moreau et al., 2013).

680 Demographic, clinical, and biochemical metadata were collected at the time of biological sampling.
681 Standard clinical composite scores used for risk stratification and prognostication included the Child-
682 Pugh score (Pugh et al., 1973), model for end-stage liver disease (MELD) (Kim et al., 2008), United
683 Kingdom model for end-stage liver disease (UKELD) (Asrani and Kim, 2010), and Chronic Liver Failure
684 Consortium-acute decompensation (CLIF-C AD) (Jalan et al., 2015). Healthy controls aged >18 years
685 (n = 40) were recruited to establish reference values for the various assays performed. Exclusion
686 criteria for healthy controls were body mass index <18 or >27; pregnancy or active breastfeeding, a
687 personal history of thrombotic or liver disease; chronic medical conditions requiring regular primary
688 or secondary care review and/or prescribed pharmacotherapies; or current use of anticoagulants,
689 platelet function inhibitors, or oral contraceptives, and no exposure to antibiotics in the previous 6
690 months.

691 **Faecal, urine and blood sample collection and preparation**

692 Plasma samples for bile acid and cytokine profiling were obtained within 24 hours of admission to
693 hospital. Blood was drawn into ethylenediaminetetraacetic acid (EDTA) containing vacuum tubes (BD
694 Vacutainer, Franklin Lakes, NJ, USA). Plasma fractions were collected from these tubes following
695 incubation at room temperature and centrifugation at 2,000 x g for 10 minutes at 4°C. Plasma aliquots
696 were stored immediately at -80°C until further analysis. Whole blood from EDTA tubes was aliquoted
697 into sterile microtubes for and stored immediately at -80°C for bacterial DNA quantification.

medRxiv preprint doi: https://doi.org/10.1101/2025.02.13.25322003; this version posted February 14, 2025. The copyright holder for this preprint (which was not certified by peer review) is the author/funder, who has granted medRxiv a license to display the preprint in perpetuity. All rights reserved. No reuse allowed without permission.

Faecal samples for 16S rRNA sequencing and calprotectin quantification were obtained within 48 hours of admission to hospital using non-treated sterile universal tubes. Faecal samples were kept at 4˚C without any preservative and within 6 hours were aliquoted into 1 gram vials for storage at -80˚C.

Serum and urine samples were prepared for NMR analyses using standardised protocols (Dona et al., 2014).

Isolation and quality assessment of faecal bacterial DNA

Bacterial DNA was isolated from all faecal samples obtained. This was performed utilising an ISOLATE II Faecal DNA Kit (Bioline, London, UK; BIO-52082). Faecal samples were thawed from -80^{o}C at room temperature for up to 30 minutes. 150mg of faecal material (crude faecal from each faecal sample) was added directly to a Bashing Beads Lysis Tube (Zymo Research, Orange County, California, USA) and rapidly lysed by bead beating in a vortex, without the use of organic denaturants or proteinases. The DNA was then bound, isolated and purified using spin columns. To optimise the DNA binding step, β-mercaptoethanol (Sigma-Aldrich, Saint Louis, Missouri, USA) was added to eliminate deoxyribonucleases released during cell lysis, by reducing the disulfide bonds within the deoxyribonuclease enzymes. This prevents enzymatic digestion of the DNA during its extraction procedure, increasing the overall yield. The eluted DNA, free of contaminants and enzyme inhibitors, is then used for downstream molecular biology applications including genotyping and sequencing. Extracted DNA concentration and purity were measured using a NanoDrop spectrophotometer (Thermo Fisher Scientific, Australia). Samples with DNA concentrations below the dynamic range of the NanoDrop spectrophotometer were analysed using Qubit High-Sensitivity (HS) dsDNA Assay kit (Life Technologies, Australia).

Faecal 16S rRNA gene amplicon library preparation and sequencing

Amplicons were generated using the method as described previously (Jervis-Bardy et al. 2015). Full details of the library preparation and sequencing protocol are provided in Appendix section 9.3. In brief, barcoded amplicon libraries for the bacterial community analysis on the Illumina MiSeq

medRxiv preprint doi: https://doi.org/10.1101/2025.02.13.25322003; this version posted February 14, 2025. The copyright holder for this preprint (which was not certified by peer review) is the author/funder, who has granted medRxiv a license to display the preprint in perpetuity. All rights reserved. No reuse allowed without permission.

platform were generated using degenerate primers targeting the V1 and V3 hypervariable regions of the bacterial 16S rRNA gene and Nextera XT index kit (Illumina, Inc., Victoria, Australia).

Amplicons were generated using fusion degenerate primers 27 F (5'-TCGTCGGCAGCGTCAGATGTGTATAAGAGACAGAGRGTTTGATCMTGGCTCAG-3') and 519R (5'-GTCTCGTGGGCTCGGAGATGTGTATAAGAGACAGGTNTTACNGCGGCKGCTG-3') with ligated overhang Illumina adapter consensus sequences in italic text. In brief, the initial PCR reactions were performed on a Veriti 96-well Thermal Cycler (Life Technologies, Australia). The PCR reactions were performed in the following programme: initiation enzyme activation at 95°C for 3 min, followed by 25 cycles consisting of denaturation at 95°C for 30 sec, annealing at 55°C for 30 sec and extension at 72°C for 30 sec. After 25 cycles, the reaction was completed with a final extension of 7 min at 72°C.

The Illumina Nextera XT Index kit (Illumina Inc., San Diego. CA, USA) with dual 8-base indices were used to allow for multiplexing. Two unique indices located on either end of the amplicon were chosen based on the Nextera dual-indexing strategy. To incorporate the indices to the 16S amplicons, PCR reactions were performed on a Veriti 96-well Thermal Cycler (Life Technologies, Australia). Cycling conditions consisted of one cycle of 95°C for 3 min, followed by eight cycles of 95°C for 30 sec, 55°C for 30 sec and 72°C for 30 sec, followed by a final extension cycle of 72°C for 5 min.

Prior to library pooling, the barcoded libraries were quantified using the Qubit dsDNA HS Assay Kit (Life Technologies, Carlsbad, CA, USA). Results from this quantification step (amplicon concentration) were used in downstream processing to eliminate contamination. The libraries were sequenced by 2 × 300 bp paired-end sequencing on the MiSeq platform using MiSeq v3 Reagent Kit (Illumina) at the Flinders Genomics Facility, Adelaide, Australia. All sequence data generated have been submitted to the Sequence Read Archive (Archive 2014).

16S rRNA amplicon sequencing analysis

The 16S rRNA amplicon sequencing raw reads are deposited in NCBI SRA under project PRJNA1223169. Sequencing reads were analysed using OTU clustering approach via QIIME v1.9.1 as

medRxiv preprint doi: https://doi.org/10.1101/2025.02.13.25322003; this version posted February 14, 2025. The copyright holder for this preprint (which was not certified by peer review) is the author/funder, who has granted medRxiv a license to display the preprint in perpetuity. All rights reserved. No reuse allowed without permission.

748 previously described (Kiu et al., 2019). Briefly, raw paired-end reads were firstly merged using PEAR
749 v0.9.6 with -q 30 option (Zhang et al., 2014). Next, quality filtering is performed with
750 split_libraries_fastq.py (QIIME) with -q 29 to retain high-quality reads (Caporaso et al., 2010).
751 Subsequently, chimera removal was performed via chimera identification
752 (identify_chimeric_seqs.py) and chimera sequence removal script (filter_fasta.py). OTU clustering
753 was run via open reference approach (pick_open_reference_otus.py) which does not discard
754 unassigned reads, based on SILVA_132 16S rRNA database optimised for use with QIIME (Quast et
755 al., 2013). BIOM outputs of taxonomic profiles generated from QIIME were then exported using
756 MEGAN v6 (Huson et al., 2016).

757 The sequencing output of 135 samples included one sample containing only 405 sequences and this
758 was discarded from further analysis. The remaining 134 samples contained a mean of 13,905
759 sequences per sample (Standard Deviation 6,497) with a minimum of 2,761 and maximum of 38,637
760 sequences per sample. Rarefaction curves were generated using the rarecurve function in the vegan
761 package (Oksanen, 2017) in R to confirm acceptable levels of sequencing depth. Raw data was
762 normalised using the Deseq2 (Love et al., 2014) package in R using the
763 varianceStabilizingTransformation function.

764 **_Enterococcus_ isolation, genomic DNA extraction, Whole Genome Sequencing (WGS) and analysis**

765 Selected faecal samples (~20mg) were subject to serial dilutions in sterile PBS before spread-plating
766 on Slanetz and Bartley agar (Thermo Scientific) for selection of Enterococcus colonies (Slanetz and
767 Bartley, 1957). Subsequently, distinct deep-red coloured colonies, presumably Enterococci, on the
768 agar plates were picked and re-streaked once on fresh Slanetz and Bartley agar after incubation at
769 40°C for 24h. Re-streaked agar plates were then incubated at 40°C for a further 24h to ensure isolate
770 purity prior to overnight culturing in 10ml Brain Heart Infusion media at 40°C to generate sizable
771 bacterial pellets for subsequent genomic DNA extraction. Genomic DNA extraction on the

medRxiv preprint doi: https://doi.org/10.1101/2025.02.13.25322003; this version posted February 14, 2025. The copyright holder for this preprint (which was not certified by peer review) is the author/funder, who has granted medRxiv a license to display the preprint in perpetuity. All rights reserved. No reuse allowed without permission.

Enterococcus isolates was performed using FastDNA Spin Kit for Soil (MP Biomedicals) as per manufacturer's instructions as described previously (Gooch et al., 2021).

Sequencing library was prepared via a modified Illumina Nextera Flex low input tagmentation approach as described previously (Baker et al., 2021; Gooch et al., 2021). Genomic DNA samples were sequenced on Illumina NextSeq 500 with read lengths of 150bp (paired-end).

Sequencing reads were quality-filtered and adapter-removed using fastp v0.20.0 with -q 20 option (Chen et al., 2018). Next, short reads were assembled using Unicycler v0.4.9 via primary de novo assembler SPAdes v3.11.1 prior to read polishing via Pilon v1.22. Contigs of length <500 bp were then removed from all draft genome assemblies (Bankevich et al., 2012; Walker et al., 2014; Wick et al., 2017). Taxonomic assignment (Enterococcus faecium) to novel draft genome assemblies were performed using GTDB-Tk v1.5.1 (Chaumeil et al., 2020).

A total of 185 E. faecium complete genome assemblies were retrieved from NCBI Genome database (December 2021) for comparison purposes. Together with 5 novel *E. faecium* genomes (n=200), a core gene alignment was generated using Panaroo v1.2.8 with --merge_paralogs option while SNP variants were next extracted by snp-sites v2.3.3 (Page et al., 2016; Tonkin-Hill et al., 2020). Subsequently, a phylogenetic tree was reconstructed via FastTree v2.1 -gtr (-nt) model based on the alignment of core genome SNPs and visualised on iTOL v6 (Letunic and Bork, 2019; Price et al., 2009).

Gene search was performed via ABRicate v1.0.1 with --mincov=90 and--minid=90, using databases ARG-ANNOT v6 (AMR genes) and VFDB (Virulence genes) (Gupta et al., 2014; Liu et al., 2019). Nucleotide sequences of bile-salt resistance genes bsh (Accession: AY260046.1) and gltK (Accession: EFF34375.1) were retrieved from GenBank (Benson et al., 2018).

Faecal calprotectin quantification

Faecal calprotectin was measured from frozen faecal samples using a commercially available enzyme-linked immunosorbent assay (Bühlmann Laboratories AG, Schönenbuch, Switzerland) that measures calprotectin in a quantitative manner. This was undertaken in a conventional hospital clinical

medRxiv preprint doi: https://doi.org/10.1101/2025.02.13.25322003; this version posted February 14, 2025. The copyright holder for this preprint (which was not certified by peer review) is the author/funder, who has granted medRxiv a license to display the preprint in perpetuity. All rights reserved. No reuse allowed without permission.

laboratory (ISO 15189 accredited) with regular interval review of standard operating procedures and equipment calibration. Extraction buffer was added to aliquots of 50mg raw faeces at a weight/volume ratio of 1:50 and homogenised by vortexing for 30 minutes. 2mL of the homogenate was then centrifuged in a microcentrifuge for 5 min at 3000 g. Following centrifugation, the calprotectin ELISA was performed using an automated Grifols Triturus® platform. The ELISA plate is coated with a monoclonal capture antibody highly specific to the calprotectin heterodimeric and polymeric complexes. After incubation, washing, a second incubation with a specific detection antibody, and a further washing step, tetramethylbenzidine (blue colour formation) followed by a stop solution (change to yellow colour) are added by the Triturus. The absorption was determined at an optical density of 450 nm. The linear range of the test was 10-600 µg calprotectin/g faeces with concentration-dependent intra- and inter-assay coefficients of between 2-5% and 4-8%, respectively.

Whole blood 16S ribosomal DNA quantification

The method for quantifying whole blood 16S ribosomal DNA has been previously published in detail (Vergis et al., 2017). Prior to 16S rRNA gene PCR analysis, frozen whole blood samples were thawed to room temperature over a 15-minute period. Mutanolysin (Sigma, St. Louis, Missouri, USA) was added directly to the whole-blood sample; 10µL of 10U/µL enzyme was added for every 200µL of blood being processed, and the sample was incubated for 30 minutes at 37°C.

DNA isolation was performed using a total whole blood volume of 200µL per sample. 19µL of 10mg/ml lysozyme and 1µL glycogen (Thermo Fisher Scientific; R0561), the latter to aid precipitation, was added to the sample and placed in a water bath at 37°C for 30 minutes. A modified protocol from the QIAmp DNA Blood Mini Kit (Qiagen, Inc., Valencia, CA) was then followed: 200µL of AL buffer was added and the sample vortexed. 20µL of Proteinase K (Thermo Fisher Scientific; EO0491) was then added and then incubated at 56°C for 1 hour in a heat block. After incubation, 200µL of 100% ethanol was added and the resulting lysates were loaded onto the QIAamp DNA Mini kit spin columns.

The columns were then centrifuged at 6,000 x g for one minute, and 500µL wash buffer AW1 added, again centrifuged at 6,000 x g for one minute. 500µL wash buffer AW2 was then added, centrifuged

medRxiv preprint doi: https://doi.org/10.1101/2025.02.13.25322003; this version posted February 14, 2025. The copyright holder for this preprint (which was not certified by peer review) is the author/funder, who has granted medRxiv a license to display the preprint in perpetuity. All rights reserved. No reuse allowed without permission.

at 13,000 x g for three minutes. 50µL of pre-warmed AE elution buffer was added with 5 minutes waiting time, then centrifuged at 13,000 x g for one minute to obtain the DNA extracts. To maximise extraction, the eluate was reapplied to the spin column and centrifuged at 6,000 x g for one minute. PBS and healthy control whole blood PCR were included to quality check for contamination from the process.

Real-time polymerase chain reaction (PCR) was used to assess the quantity of bacterial DNA by comparing to known standards. The primers and TaqMan probes were the well-characterized RW01 and DG74 primers and TaqMan RDR245 universal probe (synthesized at Applied Biosystems, Foster City, CA) and have been described previously (Jordan and Durso, 2005) with a 380bp 16S rRNA gene target. This target is located in the highly conserved region of 16S bacterial rRNA gene in order to detect the majority of bacterial species found in clinical samples.

The forward primer sequence was: 5'-AAC TGG AGG AAG GTG GGG AT3' and the reverse primer sequence was 5'-AGG AGG TGA TCC AAC CGC A-3'. The TaqMan probe sequence was 5'-(6-FAM)-TA CAA GGC CCG GGA ACG TAT TCA CCG-(TAMRA)-3'. Each well contained 5.5µL sterile water (UV irradiated), 1µL RW01 forward primer (10uM), 1µL DG74 reverse primer (10µM), 0.5ul RDR245 TaqMan probe (10µM), 10µL of TaqMan Gene Expression Master Mix (Invitrogen; 4369016) and 2µL of sample containing the DNA eluate.

A 96 well plate was used and each sample was run in triplicate, and for each plate that was run blank wells were included, a negative control (sterile PBS) and various healthy control samples spiked with a known quantity of E.coli and then serially diluted to generate a standard curve to allow absolute quantification to be calculated. Accordingly, for each PCR run, a standard curve was generated by including a healthy control blood sample which was spiked with known quantities of E.coli (0.4ng, 0.04ng, 0.004ng, 0.0004ng, 0.00004ng) using serial 10-fold dilutions and a negative control, also all run in triplicate, and were put through the same DNA extraction process. Any sample displaying a positive signal at or below the level of the negative control was considered negative. Any triplicate

medRxiv preprint doi: https://doi.org/10.1101/2025.02.13.25322003; this version posted February 14, 2025. The copyright holder for this preprint (which was not certified by peer review) is the author/funder, who has granted medRxiv a license to display the preprint in perpetuity. All rights reserved. No reuse allowed without permission.

group with readings >1 copy cycle apart was considered unreliable and discarded; otherwise, the mean reading was calculated.

A StepOnePlus PCR instrument (Invitrogen) was used for real-time PCR, with an initial 2 minutes at 50°C and 10-minute denaturation at 95°C, followed by 40 cycles of 15 seconds at 95°C, 30 seconds at 60C (annealing) and 1 minute at 72°C (extension). Fluorescence measurements on the PCR instrument were collected during the extension phase of each cycle, and a cycle threshold (C_T) value for each sample and control (including a blank well) was calculated by determining the point at which the fluorescence exceeded the threshold limit, which was set automatically. These values were compared with the *E. coli* standards to obtain a relative quantification of bacterial DNA detected in the whole blood and control samples. Standard curves were generated, and concentrations interpolated in Prism, version 7.0 (GraphPad, La Jolla, CA, USA) The results were extrapolated to picograms of bacterial DNA per millilitre of whole blood.

Plasma cytokine analyses

Plasma cytokines were measured as follows: IL-2, IL-4, IL-6, IL-8, IL-10, IL-12 p70, IL-13, IFN-ɣ, IL1β and TNF-α using an electro-chemiluminescence platform (Meso Scale Discovery (MSD)). Samples were run in duplicate on U-PLEX Proinflam Combo 1 Human™ plates (Cat# K15049K-1, MSD, Gaithersburg, MD). This was conducted according to the manufacturer's protocol. The plate was immediately read on a SECTOR(r) Imager (MSD, Gaithersburg, MD).

Plasma bile acid profiling

Bile acid (BA) profiling was done using an in-house high performance liquid chromatography tandem mass spectrometry (LC-MS/MS) assay modified from published methodology (Tagliacozzi et al., 2003). The method uses an Acentis fusedcore C18 analytical column (15064.6 mm, particle size 2.7 mm, Sigma-Aldrich) on a Jasco LC2000 series HPLC system attached to an API 3200 triple quadrupole mass spectrometer (Applied Biosystems, Cheshire, UK). Mobile phases comprised (A) methanol or (B) deionised H2O, each containing 5 mM ammonium acetate (w/v) and 0.012% formic acid (v/v).

medRxiv preprint doi: https://doi.org/10.1101/2025.02.13.25322003; this version posted February 14, 2025. The copyright holder for this preprint (which was not certified by peer review) is the author/funder, who has granted medRxiv a license to display the preprint in perpetuity. All rights reserved. No reuse allowed without permission.

Negative ion mass spectra of the fractionated BAs were recorded in multiple reaction-monitoring mode. Data were captured using Analyst Software version 1.4.2 (Applied Biosystems) and quantitation carried out by peak area analysis corrected to internal standards (a2,2,4,4,d4-deoxycholic acid for each of the bile acid chemistries; unconjugated, glycine- and taurine-conjugated). The method was linear between 0.1 and 10 mmol/L for all BAs and their conjugates with coefficients of variation (CV %) of 1.5–6.8% at the lower limit of quantitation (0.1 mmol/L). The inter-assay CV was 3.6–8.0%.

Plasma ^{1}H NMR spectroscopy

All plasma samples were prepared according to the previously published papers by Dona et al. and Trovato et al. (Dona et al., 2014; Trovato et al., 2021)[TOO ADD]. ^{1}H NMR spectra were acquired on a Bruker 600 MHz (Avance III) spectrometer, operating at a ^{1}H frequency of 600.16 MHz (14.1 Tesla) at 300K using a 5 mm BBI probe and an automated Sample Jet system (Bruker Biospin, Rheinstetten, Germany). Full explanation of processing is given in the Supplementary section.

Urine ^{1}H NMR spectroscopy

Urinary NMR data were acquired at the Centre for Biomolecular Spectroscopy, King's College London, using a Bruker 600-MHz (AVANCE NEO) NMR spectrometer with a 1H/13C/15N TCI Prodigy (nitrogen-cooled) probe (Bruker, Billerica, USA) as previously described (Bajaj et al., 2019). Pulse-collect NMR data sets were acquired using PURGE water suppression (Le Guennec et al., 2017) and J-resolved NMR sequences. Signal intensities of metabolite regions were obtained using intellibucketing within Wiley KnowItAll® Informatics, Metabolomics Edition v17.0, Wiley Science Solutions, Colorado, USA. NMR spectral regions excluded from the analysis at the outset were 10.0 ppm and 4.5-5.0 ppm (residual water region). Selected intellibucket regions were manually adjusted to incorporate specific metabolite peaks. The binned NMR spectral data outputted from Wiley KnowItAll® Informatics Metabolomics Edition v17.0 were also analysed using MetaboAnalyst v4.0 program (J et al., 2018) and exported to the Quadram Institute. Details can be found in the Supplementary section.

medRxiv preprint doi: https://doi.org/10.1101/2025.02.13.25322003; this version posted February 14, 2025. The copyright holder for this preprint (which was not certified by peer review) is the author/funder, who has granted medRxiv a license to display the preprint in perpetuity. All rights reserved. No reuse allowed without permission.

898 **Monocyte intracellular cytokine staining**

899 Monocyte intracellular cytokine staining was undertaken using thawed PBMCs from patients with
900 liver disease and at a density of 0.5 millions cells per ml. Cells were either stimulated with TLR2
901 (Pam3CSK4 5ug/ml), Invivogen, France), TLR4 (LPS 100 ng/ml), or TLR9 (CpG 10ug/ml) (Invivogen,
902 France) for 4 hours, or left unstimulated. Monocytes were identified using monoclonal antibodies for
903 surface markers: CD14 PE-Cy7, CD16 APC-H7 (BD Biosciences, UK) and HLA-DR PerCP (ThermoFisher
904 Scientific, UK). Intracellular cytokines were measured using protein transport inhibitor containing
905 monensin, permeabilization/fixation buffer and monoclonal antibodies TNF-α APC and IL-6 PE (BD
906 Biosciences, UK). Percentage positivity in CD14+ monocytes compared with isotype controls (APC
907 mouse IgG1; PE rat IgG2a) were assessed by flow cytometry as previously described (Antoniades et
908 al., 2014). The gating strategy that was employed is shown in Supplementary Figure 1.

909 **Statistical and bioinformatic analyses**

910 For microbiota diversity analysis the number of genera in each sample and the Inverse Simpson
911 diversity was calculated using the specnumber and the diversity functions on genus level taxonomic
912 sequence data in the vegan package (version 2.6-4) in R using raw sequence count data (Oksanen,
913 2017). Differences in alpha-diversity between cirrhosis severity and HC groups was tested with an
914 ANOVA using the aov function in R. Post-hoc pairwise comparisons were determined using the
915 TukeyHSD function in R.

916 To visualise clustering of gut bacterial communities between participants non-metric
917 multidimensional scaling (NMDS) based on a Bray-Curtis distance matrix and using the metaMDS
918 function with k = 3 dimensions contained within the vegan package (version 2.6-4) (Oksanen, 2017).
919 The influence of cirrhosis severity group compared to HC on participant microbiota clustering was
920 tested using a PERMANOVA test using the adonis2 function in the vegan package (version 2.6-4) with
921 a total of 10,000 permutations. Pairwise comparison of clustering of the three cirrhosis severity and
922 HC groups was compared using the pairwiseAdonis function in the pairwiseAdonis package (Martinez
923 Arbizu, 2020).

medRxiv preprint doi: https://doi.org/10.1101/2025.02.13.25322003; this version posted February 14, 2025. The copyright holder for this preprint (which was not certified by peer review) is the author/funder, who has granted medRxiv a license to display the preprint in perpetuity. All rights reserved. No reuse allowed without permission.

To explore the effect size and significance of associations between clinical metadata variables and beta-diversity of the microbiota within patient samples the envfit function in the vegan package was used to test associations of clinical metadata variables on NMDS ordination calculated using Bray-Curtis dissimilarity after 10,000 permutations. In total, 76 clinical metadata variables were included in the envfit analysis to explore their associations with the gut microbiota composition with three samples excluded during analysis due to missing data (Supplementary File 2). The P-values for combined continuous and factor variables were corrected for multiple comparisons using an FDR adjustment (Benjamini–Hochberg procedure). For visualisation the R2 for the forty significant variables were presented as a bar plot while an arbitrary top ten clinical variables explaining the highest amount of variance (R2) were plotted as an overlay on a NMDS plot of the individual gut microbiota data using the ggplot2 package.

Associations between the relative abundance of individual bacterial genera and individual clinical metadata variables were tested using the MaAsLin2 package (Mallick et al., 2021). For genus abundance analysis MaAsLin2 was run with default parameters including multiple testing correction using Benjamini-Hochberg FDR with a significance threshold on adjusted P-values of 0.25 as recommended by the developers. Exceptions to default parameters included an applied minimum prevalence of 0.01 and abundance cut-off of 0.01. Each metadata variable was tested individually. For genus differential abundance analysis cirrhosis severity was included at a Fixed Effect with the HC group as the reference group. For genus differential abundance analysis using antibiotic use, oral food intake, and lactulose use each variable was tested individually. Positive associations were identified antibiotic use, oral food intake, and lactulose and these three variables where combined and tested together as Fixed Effects in a multivariable analysis for the final analysis.

Differential analysis of bile acid concentrations was performed using MaAsLin2 with multiple testing correction using Benjamini-Hochberg FDR with a significance threshold on adjusted P-values of 0.25 as recommended by the developers. Exceptions to default parameters included no minimum concentration nor abundance cut-off, CLR as the normalisation method and no transformation used. Differential analysis of urinary metabolite and plasma concentrations were analysed using MaAsLin2

medRxiv preprint doi: https://doi.org/10.1101/2025.02.13.25322003; this version posted February 14, 2025. The copyright holder for this preprint (which was not certified by peer review) is the author/funder, who has granted medRxiv a license to display the preprint in perpetuity. All rights reserved. No reuse allowed without permission.

run with default parameters including multiple testing correction using Benjamini-Hochberg FDR with a significance threshold on adjusted P-values of 0.25 as recommended by the developers. Exceptions to default parameters included no minimum concentration nor abundance cut-off, and no normalisation nor transformation used. The BestNormalize package (version 1.9.1.9000) (Peterson, 2021; Peterson and Cavanaugh, 2020) in R was used to optimally normalise each metabolite individually before analysis using the bestnorm function. The method used to transform each variable included in (Supplementary Table 3).

For correlation analysis the variables were normalised using the bestnorm function from the bestNormalize package (version 1.9.1.9000). The method used to transform each variable included in (Supplementary Table 4). Pearson correlations were used with statistical significance corrected for multiple testing across genus tested using the False Discovery Rate method.

medRxiv preprint doi: https://doi.org/10.1101/2025.02.13.25322003; this version posted February 14, 2025. The copyright holder for this preprint (which was not certified by peer review) is the author/funder, who has granted medRxiv a license to display the preprint in perpetuity. All rights reserved. No reuse allowed without permission.

8. References

Abdugheni, R., Wang, W.-Z., Wang, Y.-J., Du, M.-X., Liu, F.-L., Zhou, N., Jiang, C.-Y., Wang, C.-Y., Wu, L., Ma, J., Liu, C., Liu, S.-J., 2022. Metabolite profiling of human-originated Lachnospiraceae at the strain level. iMeta 1, e58. https://doi.org/10.1002/imt2.58

Acharya, C., Bajaj, J.S., 2019. Altered Microbiome in Patients With Cirrhosis and Complications. Clin Gastroenterol Hepatol 17, 307–321. https://doi.org/10.1016/j.cgh.2018.08.008

Adak, A., Khan, M.R., 2019. An insight into gut microbiota and its functionalities. Cell Mol Life Sci 76, 473–493. https://doi.org/10.1007/s00018-018-2943-4

Albillos, A., de Gottardi, A., Rescigno, M., 2020. The gut-liver axis in liver disease: Pathophysiological basis for therapy. J Hepatol 72, 558–577. https://doi.org/10.1016/j.jhep.2019.10.003

Albillos, A., Martin-Mateos, R., Van der Merwe, S., Wiest, R., Jalan, R., Álvarez-Mon, M., 2022. Cirrhosis-associated immune dysfunction. Nat Rev Gastroenterol Hepatol 19, 112–134. https://doi.org/10.1038/s41575-021-00520-7

Alexopoulou, A., Agiasotelli, D., Vasilieva, L.E., Dourakis, S.P., 2017. Bacterial translocation markers in liver cirrhosis. Ann Gastroenterol 30, 486–497. https://doi.org/10.20524/aog.2017.0178

Antoniades, C.G., Khamri, W., Abeles, R.D., Taams, L.S., Triantafyllou, E., Possamai, L.A., Bernsmeier, C., Mitry, R.R., O'Brien, A., Gilroy, D., Goldin, R., Heneghan, M., Heaton, N., Jassem, W., Bernal, W., Vergani, D., Ma, Y., Quaglia, A., Wendon, J., Thursz, M., 2014. Secretory leukocyte protease inhibitor: a pivotal mediator of anti-inflammatory responses in acetaminophen-induced acute liver failure. Hepatology 59, 1564–1576. https://doi.org/10.1002/hep.26933

Arroyo, V., Moreau, R., Jalan, R., Ginès, P., EASL-CLIF Consortium CANONIC Study, 2015. Acute-on-chronic liver failure: A new syndrome that will re-classify cirrhosis. J Hepatol 62, S131-143. https://doi.org/10.1016/j.jhep.2014.11.045

Arroyo, V., Moreau, R., Kamath, P.S., Jalan, R., Ginès, P., Nevens, F., Fernández, J., To, U., García-Tsao, G., Schnabl, B., 2016. Acute-on-chronic liver failure in cirrhosis. Nat Rev Dis Primers 2, 16041. https://doi.org/10.1038/nrdp.2016.41

Asrani, S.K., Kim, W.R., 2010. Organ allocation for chronic liver disease: model for end-stage liver disease and beyond. Curr Opin Gastroenterol 26, 209–213. https://doi.org/10.1097/MOG.0b013e32833867d8

Bach Knudsen, K.E., Lærke, H.N., Hedemann, M.S., Nielsen, T.S., Ingerslev, A.K., Gundelund Nielsen, D.S., Theil, P.K., Purup, S., Hald, S., Schioldan, A.G., Marco, M.L., Gregersen, S., Hermansen, K., 2018. Impact of Diet-Modulated Butyrate Production on Intestinal Barrier Function and Inflammation. Nutrients 10, 1499. https://doi.org/10.3390/nu10101499

Bajaj, J.S., Heuman, D.M., Hylemon, P.B., Sanyal, A.J., White, M.B., Monteith, P., Noble, N.A., Unser, A.B., Daita, K., Fisher, A.R., Sikaroodi, M., Gillevet, P.M., 2014. Altered profile of human gut microbiome is associated with cirrhosis and its complications. Journal of Hepatology 60, 940–947. https://doi.org/10.1016/j.jhep.2013.12.019

Bajaj, J.S., Reddy, K.R., Tandon, P., Garcia-Tsao, G., Kamath, P.S., O'Leary, J.G., Wong, F., Lai, J., Vargas, H., Thuluvath, P.J., Subramanian, R.M., Pena-Rodriguez, M., Sikaroodi, M., Thacker, L.R.,

medRxiv preprint doi: https://doi.org/10.1101/2025.02.13.25322003; this version posted February 14, 2025. The copyright holder for this preprint (which was not certified by peer review) is the author/funder, who has granted medRxiv a license to display the preprint in perpetuity. All rights reserved. No reuse allowed without permission.

1005 Gillevet, P.M., 2022. Association of serum metabolites and gut microbiota at hospital
1006 admission with nosocomial infection development in patients with cirrhosis. Liver Transpl 28,
1007 1831–1840. https://doi.org/10.1002/lt.26552
1008 Bajaj, J.S., Ridlon, J.M., Hylemon, P.B., Thacker, L.R., Heuman, D.M., Smith, S., Sikaroodi, M., Gillevet,
1009 P.M., 2012. Linkage of gut microbiome with cognition in hepatic encephalopathy. Am J Physiol
1010 Gastrointest Liver Physiol 302, G168-175. https://doi.org/10.1152/ajpgi.00190.2011
1011 Bajaj, J.S., Salzman, N., Acharya, C., Takei, H., Kakiyama, G., Fagan, A., White, M.B., Gavis, E.A., Holtz,
1012 M.L., Hayward, M., Nittono, H., Hylemon, P.B., Cox, I.J., Williams, R., Taylor-Robinson, S.D.,
1013 Sterling, R.K., Matherly, S.C., Fuchs, M., Lee, H., Puri, P., Stravitz, R.T., Sanyal, A.J., Ajayi, L., Le
1014 Guennec, A., Atkinson, R.A., Siddiqui, M.S., Luketic, V., Pandak, W.M., Sikaroodi, M., Gillevet,
1015 P.M., 2019. Microbial functional change is linked with clinical outcomes after capsular fecal
1016 transplant in cirrhosis. JCI Insight 4, e133410, 133410.
1017 https://doi.org/10.1172/jci.insight.133410
1018 Baker, D.J., Aydin, A., Le-Viet, T., Kay, G.L., Rudder, S., de Oliveira Martins, L., Tedim, A.P., Kolyva, A.,
1019 Diaz, M., Alikhan, N.-F., Meadows, L., Bell, A., Gutierrez, A.V., Trotter, A.J., Thomson, N.M.,
1020 Gilroy, R., Griffith, L., Adriaenssens, E.M., Stanley, R., Charles, I.G., Elumogo, N., Wain, J.,
1021 Prakash, R., Meader, E., Mather, A.E., Webber, M.A., Dervisevic, S., Page, A.J., O'Grady, J.,
1022 2021. CoronaHiT: high-throughput sequencing of SARS-CoV-2 genomes. Genome Medicine
1023 13, 21. https://doi.org/10.1186/s13073-021-00839-5
1024 Bankevich, A., Nurk, S., Antipov, D., Gurevich, A.A., Dvorkin, M., Kulikov, A.S., Lesin, V.M., Nikolenko,
1025 S.I., Pham, S., Prjibelski, A.D., Pyshkin, A.V., Sirotkin, A.V., Vyahhi, N., Tesler, G., Alekseyev,
1026 M.A., Pevzner, P.A., 2012. SPAdes: a new genome assembly algorithm and its applications to
1027 single-cell sequencing. J Comput Biol 19, 455–477. https://doi.org/10.1089/cmb.2012.0021
1028 Benson, D.A., Cavanaugh, M., Clark, K., Karsch-Mizrachi, I., Ostell, J., Pruitt, K.D., Sayers, E.W., 2018.
1029 GenBank. Nucleic Acids Research 46, D41–D47. https://doi.org/10.1093/nar/gkx1094
1030 Caballero-Flores, G., Pickard, J.M., Núñez, G., 2023. Microbiota-mediated colonization resistance:
1031 mechanisms and regulation. Nat Rev Microbiol 21, 347–360. https://doi.org/10.1038/s41579-
1032 022-00833-7
1033 Caporaso, J.G., Kuczynski, J., Stombaugh, J., Bittinger, K., Bushman, F.D., Costello, E.K., Fierer, N.,
1034 Peña, A.G., Goodrich, J.K., Gordon, J.I., Huttley, G.A., Kelley, S.T., Knights, D., Koenig, J.E., Ley,
1035 R.E., Lozupone, C.A., McDonald, D., Muegge, B.D., Pirrung, M., Reeder, J., Sevinsky, J.R.,
1036 Turnbaugh, P.J., Walters, W.A., Widmann, J., Yatsunenko, T., Zaneveld, J., Knight, R., 2010.
1037 QIIME allows analysis of high-throughput community sequencing data. Nat Methods 7, 335–
1038 336. https://doi.org/10.1038/nmeth.f.303
1039 Chaumeil, P.-A., Mussig, A.J., Hugenholtz, P., Parks, D.H., 2020. GTDB-Tk: a toolkit to classify genomes
1040 with the Genome Taxonomy Database. Bioinformatics 36, 1925–1927.
1041 https://doi.org/10.1093/bioinformatics/btz848
1042 Chen, S., Zhou, Y., Chen, Y., Gu, J., 2018. fastp: an ultra-fast all-in-one FASTQ preprocessor.
1043 Bioinformatics 34, i884–i890. https://doi.org/10.1093/bioinformatics/bty560

medRxiv preprint doi: https://doi.org/10.1101/2025.02.13.25322003; this version posted February 14, 2025. The copyright holder for this preprint (which was not certified by peer review) is the author/funder, who has granted medRxiv a license to display the preprint in perpetuity. All rights reserved. No reuse allowed without permission.

Cibulková, I., Řehořová, V., Hajer, J., Duška, F., 2021. Fecal Microbial Transplantation in Critically Ill Patients—Structured Review and Perspectives. Biomolecules 11, 1459. https://doi.org/10.3390/biom11101459

Da Silva, H.E., Teterina, A., Comelli, E.M., Taibi, A., Arendt, B.M., Fischer, S.E., Lou, W., Allard, J.P., 2018. Nonalcoholic fatty liver disease is associated with dysbiosis independent of body mass index and insulin resistance. Sci Rep 8, 1466. https://doi.org/10.1038/s41598-018-19753-9

D'Amico, G., Bernardi, M., Angeli, P., 2022. Towards a new definition of decompensated cirrhosis. Journal of Hepatology 76, 202–207. https://doi.org/10.1016/j.jhep.2021.06.018

Dona, A.C., Jiménez, B., Schäfer, H., Humpfer, E., Spraul, M., Lewis, M.R., Pearce, J.T.M., Holmes, E., Lindon, J.C., Nicholson, J.K., 2014. Precision high-throughput proton NMR spectroscopy of human urine, serum, and plasma for large-scale metabolic phenotyping. Anal Chem 86, 9887–9894. https://doi.org/10.1021/ac5025039

Dubinkina, V.B., Tyakht, A.V., Odintsova, V.Y., Yarygin, K.S., Kovarsky, B.A., Pavlenko, A.V., Ischenko, D.S., Popenko, A.S., Alexeev, D.G., Taraskina, A.Y., Nasyrova, R.F., Krupitsky, E.M., Shalikiani, N.V., Bakulin, I.G., Shcherbakov, P.L., Skorodumova, L.O., Larin, A.K., Kostryukova, E.S., Abdulkhakov, R.A., Abdulkhakov, S.R., Malanin, S.Y., Ismagilova, R.K., Grigoryeva, T.V., Ilina, E.N., Govorun, V.M., 2017. Links of gut microbiota composition with alcohol dependence syndrome and alcoholic liver disease. Microbiome 5, 141. https://doi.org/10.1186/s40168-017-0359-2

European Association for the Study of the Liver., 2018. EASL Clinical Practice Guidelines for the management of patients with decompensated cirrhosis. J Hepatol 69, 406–460. https://doi.org/10.1016/j.jhep.2018.03.024

Fagan, K.J., Rogers, G.B., Melino, M., Arthur, D.M., Costello, M.-E., Morrison, M., Powell, E.E., Irvine, K.M., 2015. Ascites Bacterial Burden and Immune Cell Profile Are Associated with Poor Clinical Outcomes in the Absence of Overt Infection. PLoS One 10, e0120642. https://doi.org/10.1371/journal.pone.0120642

Flint, H.J., Scott, K.P., Duncan, S.H., Louis, P., Forano, E., 2012. Microbial degradation of complex carbohydrates in the gut. Gut Microbes 3, 289–306. https://doi.org/10.4161/gmic.19897

Garrett, W.S., 2020. Enterococcus in Graft-versus-Host Disease. N Engl J Med 382, 1064–1066. https://doi.org/10.1056/NEJMcibr1915978

Gatarek, P., Kaluzna-Czaplinska, J., 2021. Trimethylamine N-oxide (TMAO) in human health. EXCLI J 20, 301–319. https://doi.org/10.17179/excli2020-3239

Ghosh, S., Whitley, C.S., Haribabu, B., Jala, V.R., 2021. Regulation of Intestinal Barrier Function by Microbial Metabolites. Cellular and Molecular Gastroenterology and Hepatology 11, 1463–1482. https://doi.org/10.1016/j.jcmgh.2021.02.007

Gooch, H.C.C., Kiu, R., Rudder, S., Baker, D.J., Hall, L.J., Maxwell, A., 2021. Enterococcus innesii sp. nov., isolated from the wax moth Galleria mellonella. Int J Syst Evol Microbiol 71, 005168. https://doi.org/10.1099/ijsem.0.005168

Gupta, S.K., Padmanabhan, B.R., Diene, S.M., Lopez-Rojas, R., Kempf, M., Landraud, L., Rolain, J.-M., 2014. ARG-ANNOT, a New Bioinformatic Tool To Discover Antibiotic Resistance Genes in

medRxiv preprint doi: https://doi.org/10.1101/2025.02.13.25322003; this version posted February 14, 2025. The copyright holder for this preprint (which was not certified by peer review) is the author/funder, who has granted medRxiv a license to display the preprint in perpetuity. All rights reserved. No reuse allowed without permission.

Bacterial Genomes. Antimicrob Agents Chemother 58, 212–220. https://doi.org/10.1128/AAC.01310-13

Hendrickx, A.P.A., van Luit-Asbroek, M., Schapendonk, C.M.E., van Wamel, W.J.B., Braat, J.C., Wijnands, L.M., Bonten, M.J.M., Willems, R.J.L., 2009. SgrA, a nidogen-binding LPXTG surface adhesin implicated in biofilm formation, and EcbA, a collagen binding MSCRAMM, are two novel adhesins of hospital-acquired Enterococcus faecium. Infect Immun 77, 5097–5106. https://doi.org/10.1128/IAI.00275-09

Hernaez, R., Solà, E., Moreau, R., Ginès, P., 2017. Acute-on-chronic liver failure: an update. Gut 66, 541–553. https://doi.org/10.1136/gutjnl-2016-312670

Horvatits, T., Drolz, A., Roedl, K., Rutter, K., Ferlitsch, A., Fauler, G., Trauner, M., Fuhrmann, V., 2017. Serum bile acids as marker for acute decompensation and acute-on-chronic liver failure in patients with non-cholestatic cirrhosis. Liver Int 37, 224–231. https://doi.org/10.1111/liv.13201

Hsu, C.L., Schnabl, B., 2023. The gut–liver axis and gut microbiota in health and liver disease. Nat Rev Microbiol 21, 719–733. https://doi.org/10.1038/s41579-023-00904-3

Huang, D.Q., Terrault, N.A., Tacke, F., Gluud, L.L., Arrese, M., Bugianesi, E., Loomba, R., 2023. Global epidemiology of cirrhosis — aetiology, trends and predictions. Nat Rev Gastroenterol Hepatol 20, 388–398. https://doi.org/10.1038/s41575-023-00759-2

Hufnagel, M., Liese, C., Loescher, C., Kunze, M., Proempeler, H., Berner, R., Krueger, M., 2007. Enterococcal colonization of infants in a neonatal intensive care unit: associated predictors, risk factors and seasonal patterns. BMC Infect Dis 7, 107. https://doi.org/10.1186/1471-2334-7-107

Huson, D.H., Beier, S., Flade, I., Górska, A., El-Hadidi, M., Mitra, S., Ruscheweyh, H.-J., Tappu, R., 2016. MEGAN Community Edition - Interactive Exploration and Analysis of Large-Scale Microbiome Sequencing Data. PLOS Computational Biology 12, e1004957. https://doi.org/10.1371/journal.pcbi.1004957

J, C., O, S., C, L., I, C., S, L., G, B., Ds, W., J, X., 2018. MetaboAnalyst 4.0: towards more transparent and integrative metabolomics analysis. Nucleic acids research 46. https://doi.org/10.1093/nar/gky310

Jalan, R., Pavesi, M., Saliba, F., Amorós, A., Fernandez, J., Holland-Fischer, P., Sawhney, R., Mookerjee, R., Caraceni, P., Moreau, R., Ginès, P., Durand, F., Angeli, P., Alessandria, C., Laleman, W., Trebicka, J., Samuel, D., Zeuzem, S., Gustot, T., Gerbes, A.L., Wendon, J., Bernardi, M., Arroyo, V., CANONIC Study Investigators; EASL-CLIF Consortium, 2015. The CLIF Consortium Acute Decompensation score (CLIF-C ADs) for prognosis of hospitalised cirrhotic patients without acute-on-chronic liver failure. J Hepatol 62, 831–840. https://doi.org/10.1016/j.jhep.2014.11.012

Jin, M., Kalainy, S., Baskota, N., Chiang, D., Deehan, E.C., McDougall, C., Tandon, P., Martínez, I., Cervera, C., Walter, J., Abraldes, J.G., 2019. Faecal microbiota from patients with cirrhosis has a low capacity to ferment non-digestible carbohydrates into short-chain fatty acids. Liver Int 39, 1437–1447. https://doi.org/10.1111/liv.14106

medRxiv preprint doi: https://doi.org/10.1101/2025.02.13.25322003; this version posted February 14, 2025. The copyright holder for this preprint (which was not certified by peer review) is the author/funder, who has granted medRxiv a license to display the preprint in perpetuity. All rights reserved. No reuse allowed without permission.

Jordan, J.A., Durso, M.B., 2005. Real-time polymerase chain reaction for detecting bacterial DNA directly from blood of neonates being evaluated for sepsis. J Mol Diagn 7, 575–581. https://doi.org/10.1016/S1525-1578(10)60590-9

Kakiyama, G., Muto, A., Takei, H., Nittono, H., Murai, T., Kurosawa, T., Hofmann, A.F., Pandak, W.M., Bajaj, J.S., 2014. A simple and accurate HPLC method for fecal bile acid profile in healthy and cirrhotic subjects: validation by GC-MS and LC-MS. J Lipid Res 55, 978–990. https://doi.org/10.1194/jlr.D047506

Kakiyama, G., Pandak, W.M., Gillevet, P.M., Hylemon, P.B., Heuman, D.M., Daita, K., Takei, H., Muto, A., Nittono, H., Ridlon, J.M., White, M.B., Noble, N.A., Monteith, P., Fuchs, M., Thacker, L.R., Sikaroodi, M., Bajaj, J.S., 2013. Modulation of the fecal bile acid profile by gut microbiota in cirrhosis. J Hepatol 58, 949–955. https://doi.org/10.1016/j.jhep.2013.01.003

Katoonizadeh, A., Laleman, W., Verslype, C., Wilmer, A., Maleux, G., Roskams, T., Nevens, F., 2010. Early features of acute-on-chronic alcoholic liver failure: a prospective cohort study. Gut 59, 1561–1569. https://doi.org/10.1136/gut.2009.189639

Kim, W.R., Biggins, S.W., Kremers, W.K., Wiesner, R.H., Kamath, P.S., Benson, J.T., Edwards, E., Therneau, T.M., 2008. Hyponatremia and mortality among patients on the liver-transplant waiting list. N Engl J Med 359, 1018–1026. https://doi.org/10.1056/NEJMoa0801209

Kiu, R., Brown, J., Bedwell, H., Leclaire, C., Caim, S., Pickard, D., Dougan, G., Dixon, R.A., Hall, L.J., 2019. Genomic analysis on broiler-associated Clostridium perfringens strains and exploratory caecal microbiome investigation reveals key factors linked to poultry necrotic enteritis. Animal Microbiome 1, 12. https://doi.org/10.1186/s42523-019-0015-1

Le Guennec, A., Tayyari, F., Edison, A.S., 2017. Alternatives to Nuclear Overhauser Enhancement Spectroscopy Presat and Carr-Purcell-Meiboom-Gill Presat for NMR-Based Metabolomics. Anal Chem 89, 8582–8588. https://doi.org/10.1021/acs.analchem.7b02354

Lee, S., Arefaine, B., Begum, N., Stamouli, M., Witherden, E., Mohamad, M., Harzandi, A., Zamalloa, A., Cai, H., Williams, R., Curtis, M., Edwards, L.A., Chokshi, S., Mardinoglu, A., Proctor, G., Moyes, D., McPhail, M.J., Shawcross, D.L., Uhlen, M., Shoaie, S., Patel, V.C., 2024a. Oral-gut microbiome interactions in advanced cirrhosis: characterisation of pathogenic enterotypes and salivatypes, virulence factors and antimicrobial. J Hepatol S0168-8278(24)02635–7. https://doi.org/10.1016/j.jhep.2024.09.046

Lee, S., Arefaine, B., Begum, N., Stamouli, M., Witherden, E., Mohamad, M., Harzandi, A., Zamalloa, A., Cai, H., Williams, R., Curtis, M.A., Edwards, L.A., Chokshi, S., Mardinoglu, A., Proctor, G., Moyes, D.L., McPhail, M.J., Shawcross, D.L., Uhlen, M., Shoaie, S., Patel, V.C., 2024b. Oral-gut microbiome interactions in advanced cirrhosis: characterisation of pathogenic enterotypes and salivatypes, virulence factors and antimicrobial resistance. Journal of Hepatology 0. https://doi.org/10.1016/j.jhep.2024.09.046

Lees, H.J., Swann, J.R., Wilson, I.D., Nicholson, J.K., Holmes, E., 2013. Hippurate: the natural history of a mammalian-microbial cometabolite. J Proteome Res 12, 1527–1546. https://doi.org/10.1021/pr300900b

Letunic, I., Bork, P., 2019. Interactive Tree Of Life (iTOL) v4: recent updates and new developments. Nucleic Acids Research 47, W256–W259. https://doi.org/10.1093/nar/gkz239

medRxiv preprint doi: https://doi.org/10.1101/2025.02.13.25322003; this version posted February 14, 2025. The copyright holder for this preprint (which was not certified by peer review) is the author/funder, who has granted medRxiv a license to display the preprint in perpetuity. All rights reserved. No reuse allowed without permission.

Liu, B., Zheng, D., Jin, Q., Chen, L., Yang, J., 2019. VFDB 2019: a comparative pathogenomic platform with an interactive web interface. Nucleic Acids Research 47, D687–D692. https://doi.org/10.1093/nar/gky1080

Love, M.I., Huber, W., Anders, S., 2014. Moderated estimation of fold change and dispersion for RNA-seq data with DESeq2. Genome Biol 15, 550. https://doi.org/10.1186/s13059-014-0550-8

Mallick, H., Rahnavard, A., McIver, L.J., Ma, S., Zhang, Y., Nguyen, L.H., Tickle, T.L., Weingart, G., Ren, B., Schwager, E.H., Chatterjee, S., Thompson, K.N., Wilkinson, J.E., Subramanian, A., Lu, Y., Waldron, L., Paulson, J.N., Franzosa, E.A., Bravo, H.C., Huttenhower, C., 2021. Multivariable association discovery in population-scale meta-omics studies. PLOS Computational Biology 17, e1009442. https://doi.org/10.1371/journal.pcbi.1009442

Martinez Arbizu, P., 2020. pairwiseAdonis: Pairwise multilevel comparison using adonis.

Moreau, R., Jalan, R., Gines, P., Pavesi, M., Angeli, P., Cordoba, J., Durand, F., Gustot, T., Saliba, F., Domenicali, M., Gerbes, A., Wendon, J., Alessandria, C., Laleman, W., Zeuzem, S., Trebicka, J., Bernardi, M., Arroyo, V., CANONIC Study Investigators of the EASL–CLIF Consortium, 2013. Acute-on-chronic liver failure is a distinct syndrome that develops in patients with acute decompensation of cirrhosis. Gastroenterology 144, 1426–1437, 1437.e1–9. https://doi.org/10.1053/j.gastro.2013.02.042

Moubareck, C., Gavini, F., Vaugien, L., Butel, M.J., Doucet-Populaire, F., 2005. Antimicrobial susceptibility of bifidobacteria. J Antimicrob Chemother 55, 38–44. https://doi.org/10.1093/jac/dkh495

Mouzaki, M., Wang, A.Y., Bandsma, R., Comelli, E.M., Arendt, B.M., Zhang, L., Fung, S., Fischer, S.E., McGilvray, I.G., Allard, J.P., 2016. Bile Acids and Dysbiosis in Non-Alcoholic Fatty Liver Disease. PLoS One 11, e0151829. https://doi.org/10.1371/journal.pone.0151829

Nallapareddy, S.R., Singh, K.V., Okhuysen, P.C., Murray, B.E., 2008. A functional collagen adhesin gene, acm, in clinical isolates of Enterococcus faecium correlates with the recent success of this emerging nosocomial pathogen. Infect Immun 76, 4110–4119. https://doi.org/10.1128/IAI.00375-08

Odenwald, M.A., Lin, H., Lehmann, C., Dylla, N.P., Cole, C.G., Mostad, J.D., Pappas, T.E., Ramaswamy, R., Moran, A., Hutchison, A.L., Stutz, M.R., Dela Cruz, M., Adler, E., Boissiere, J., Khalid, M., Cantoral, J., Haro, F., Oliveira, R.A., Waligurski, E., Cotter, T.G., Light, S.H., Beavis, K.G., Sundararajan, A., Sidebottom, A.M., Reddy, K.G., Paul, S., Pillai, A., Te, H.S., Rinella, M.E., Charlton, M.R., Pamer, E.G., Aronsohn, A.I., 2023. Bifidobacteria metabolize lactulose to optimize gut metabolites and prevent systemic infection in patients with liver disease. Nat Microbiol 1–17. https://doi.org/10.1038/s41564-023-01493-w

Oksanen, F., 2017. Vegan: Community Ecology Package.

Organ, C.L., Li, Z., Sharp, T.E., Polhemus, D.J., Gupta, N., Goodchild, T.T., Tang, W.H.W., Hazen, S.L., Lefer, D.J., 2020. Nonlethal Inhibition of Gut Microbial Trimethylamine N-oxide Production Improves Cardiac Function and Remodeling in a Murine Model of Heart Failure. Journal of the American Heart Association 9, e016223. https://doi.org/10.1161/JAHA.119.016223

medRxiv preprint doi: https://doi.org/10.1101/2025.02.13.25322003; this version posted February 14, 2025. The copyright holder for this preprint (which was not certified by peer review) is the author/funder, who has granted medRxiv a license to display the preprint in perpetuity. All rights reserved. No reuse allowed without permission.

Page, A.J., Taylor, B., Delaney, A.J., Soares, J., Seemann, T., Keane, J.A., Harris, S.R., 2016. SNP-sites: rapid efficient extraction of SNPs from multi-FASTA alignments. Microb Genom 2, e000056. https://doi.org/10.1099/mgen.0.000056

Pallister, T., Jackson, M.A., Martin, T.C., Zierer, J., Jennings, A., Mohney, R.P., MacGregor, A., Steves, C.J., Cassidy, A., Spector, T.D., Menni, C., 2017. Hippurate as a metabolomic marker of gut microbiome diversity: Modulation by diet and relationship to metabolic syndrome. Sci Rep 7, 13670. https://doi.org/10.1038/s41598-017-13722-4

Peterson, R.A., 2021. Finding Optimal Normalizing Transformations via bestNormalize. The R Journal 13, 310–329.

Peterson, R.A., Cavanaugh, J.E., 2020. Ordered quantile normalization: a semiparametric transformation built for the cross-validation era. Journal of Applied Statistics 47, 2312–2327. https://doi.org/10.1080/02664763.2019.1630372

Piano, S., Singh, V., Caraceni, P., Maiwall, R., Alessandria, C., Fernandez, J., Soares, E.C., Kim, D.J., Kim, S.E., Marino, M., Vorobioff, J., Barea, R. de C.R., Merli, M., Elkrief, L., Vargas, V., Krag, A., Singh, S.P., Lesmana, L.A., Toledo, C., Marciano, S., Verhelst, X., Wong, F., Intagliata, N., Rabinowich, L., Colombato, L., Kim, S.G., Gerbes, A., Durand, F., Roblero, J.P., Bhamidimarri, K.R., Boyer, T.D., Maevskaya, M., Fassio, E., Kim, H.S., Hwang, J.S., Gines, P., Gadano, A., Sarin, S.K., Angeli, P., International Club of Ascites Global Study Group, 2019. Epidemiology and Effects of Bacterial Infections in Patients With Cirrhosis Worldwide. Gastroenterology 156, 1368-1380.e10. https://doi.org/10.1053/j.gastro.2018.12.005

Price, M.N., Dehal, P.S., Arkin, A.P., 2009. FastTree: Computing Large Minimum Evolution Trees with Profiles instead of a Distance Matrix. Molecular Biology and Evolution 26, 1641–1650. https://doi.org/10.1093/molbev/msp077

Pugh, R.N., Murray-Lyon, I.M., Dawson, J.L., Pietroni, M.C., Williams, R., 1973. Transection of the oesophagus for bleeding oesophageal varices. Br J Surg 60, 646–649. https://doi.org/10.1002/bjs.1800600817

Quast, C., Pruesse, E., Yilmaz, P., Gerken, J., Schweer, T., Yarza, P., Peplies, J., Glöckner, F.O., 2013. The SILVA ribosomal RNA gene database project: improved data processing and web-based tools. Nucleic Acids Research 41, D590–D596. https://doi.org/10.1093/nar/gks1219

Ridlon, J.M., Alves, J.M., Hylemon, P.B., Bajaj, J.S., 2013. Cirrhosis, bile acids and gut microbiota: unraveling a complex relationship. Gut Microbes 4, 382–387. https://doi.org/10.4161/gmic.25723

Riva, A., Gray, E.H., Azarian, S., Zamalloa, A., McPhail, M.J.W., Vincent, R.P., Williams, R., Chokshi, S., Patel, V.C., Edwards, L.A., 2020. Faecal cytokine profiling as a marker of intestinal inflammation in acutely decompensated cirrhosis. JHEP Rep 2, 100151. https://doi.org/10.1016/j.jhepr.2020.100151

Seishima, J., Iida, N., Kitamura, K., Yutani, M., Wang, Z., Seki, A., Yamashita, Taro, Sakai, Y., Honda, M., Yamashita, Tatsuya, Kagaya, T., Shirota, Y., Fujinaga, Y., Mizukoshi, E., Kaneko, S., 2019. Gut-derived Enterococcus faecium from ulcerative colitis patients promotes colitis in a genetically susceptible mouse host. Genome Biol 20, 252. https://doi.org/10.1186/s13059-019-1879-9

medRxiv preprint doi: https://doi.org/10.1101/2025.02.13.25322003; this version posted February 14, 2025. The copyright holder for this preprint (which was not certified by peer review) is the author/funder, who has granted medRxiv a license to display the preprint in perpetuity. All rights reserved. No reuse allowed without permission.

Shah, N.J., Mousa, O.Y., Syed, K., John, S., 2024. Acute on Chronic Liver Failure, in: StatPearls. StatPearls Publishing, Treasure Island (FL).

Slanetz, L.W., Bartley, C.H., 1957. NUMBERS OF ENTEROCOCCI IN WATER, SEWAGE, AND FECES DETERMINED BY THE MEMBRANE FILTER TECHNIQUE WITH AN IMPROVED MEDIUM1. J Bacteriol 74, 591–595.

Solé, C., Guilly, S., Da Silva, K., Llopis, M., Le-Chatelier, E., Huelin, P., Carol, M., Moreira, R., Fabrellas, N., De Prada, G., Napoleone, L., Graupera, I., Pose, E., Juanola, A., Borruel, N., Berland, M., Toapanta, D., Casellas, F., Guarner, F., Doré, J., Solà, E., Ehrlich, S.D., Ginès, P., 2021. Alterations in Gut Microbiome in Cirrhosis as Assessed by Quantitative Metagenomics: Relationship With Acute-on-Chronic Liver Failure and Prognosis. Gastroenterology 160, 206-218.e13. https://doi.org/10.1053/j.gastro.2020.08.054

Tagliacozzi, D., Mozzi, A.F., Casetta, B., Bertucci, P., Bernardini, S., Di Ilio, C., Urbani, A., Federici, G., 2003. Quantitative analysis of bile acids in human plasma by liquid chromatography-electrospray tandem mass spectrometry: a simple and rapid one-step method. Clin Chem Lab Med 41, 1633–1641. https://doi.org/10.1515/CCLM.2003.247

Tilg, H., Adolph, T.E., Trauner, M., 2022. Gut-liver axis: Pathophysiological concepts and clinical implications. Cell Metab 34, 1700–1718. https://doi.org/10.1016/j.cmet.2022.09.017

Toledo, C., Salmerón, J.M., Rimola, A., Navasa, M., Arroyo, V., Llach, J., Ginès, A., Ginès, P., Rodés, J., 1993. Spontaneous bacterial peritonitis in cirrhosis: predictive factors of infection resolution and survival in patients treated with cefotaxime. Hepatology 17, 251–257.

Tonkin-Hill, G., MacAlasdair, N., Ruis, C., Weimann, A., Horesh, G., Lees, J.A., Gladstone, R.A., Lo, S., Beaudoin, C., Floto, R.A., Frost, S.D.W., Corander, J., Bentley, S.D., Parkhill, J., 2020. Producing polished prokaryotic pangenomes with the Panaroo pipeline. Genome Biology 21, 180. https://doi.org/10.1186/s13059-020-02090-4

Tranah, T.H., Edwards, L.A., Schnabl, B., Shawcross, D.L., 2021. Targeting the gut-liver-immune axis to treat cirrhosis. Gut 70, 982–994. https://doi.org/10.1136/gutjnl-2020-320786

Trebicka, J., Fernandez, J., Papp, M., Caraceni, P., Laleman, W., Gambino, C., Giovo, I., Uschner, F.E., Jansen, C., Jimenez, C., Mookerjee, R., Gustot, T., Albillos, A., Bañares, R., Jarcuska, P., Steib, C., Reiberger, T., Acevedo, J., Gatti, P., Shawcross, D.L., Zeuzem, S., Zipprich, A., Piano, S., Berg, T., Bruns, T., Danielsen, K.V., Coenraad, M., Merli, M., Stauber, R., Zoller, H., Ramos, J.P., Solé, C., Soriano, G., de Gottardi, A., Gronbaek, H., Saliba, F., Trautwein, C., Kani, H.T., Francque, S., Ryder, S., Nahon, P., Romero-Gomez, M., Van Vlierberghe, H., Francoz, C., Manns, M., Garcia-Lopez, E., Tufoni, M., Amoros, A., Pavesi, M., Sanchez, C., Praktiknjo, M., Curto, A., Pitarch, C., Putignano, A., Moreno, E., Bernal, W., Aguilar, F., Clària, J., Ponzo, P., Vitalis, Z., Zaccherini, G., Balogh, B., Gerbes, A., Vargas, V., Alessandria, C., Bernardi, M., Ginès, P., Moreau, R., Angeli, P., Jalan, R., Arroyo, V., PREDICT STUDY group of the EASL-CLIF CONSORTIUM, 2021. PREDICT identifies precipitating events associated with the clinical course of acutely decompensated cirrhosis. J Hepatol 74, 1097–1108. https://doi.org/10.1016/j.jhep.2020.11.019

Trovato, F.M., Zia, R., Napoli, S., Wolfer, K., Huang, X., Morgan, P.E., Husbyn, H., Elgosbi, M., Lucangeli, M., Miquel, R., Wilson, I., Heaton, N.D., Heneghan, M.A., Auzinger, G., Antoniades, C.G., Wendon, J.A., Patel, V.C., Coen, M., Triantafyllou, E., McPhail, M.J., 2021. Dysregulation

medRxiv preprint doi: https://doi.org/10.1101/2025.02.13.25322003; this version posted February 14, 2025. The copyright holder for this preprint (which was not certified by peer review) is the author/funder, who has granted medRxiv a license to display the preprint in perpetuity. All rights reserved. No reuse allowed without permission.

of the Lysophosphatidylcholine/Autotaxin/Lysophosphatidic Acid Axis in Acute-on-Chronic Liver Failure Is Associated With Mortality and Systemic Inflammation by Lysophosphatidic Acid-Dependent Monocyte Activation. Hepatology 74, 907–925. https://doi.org/10.1002/hep.31738

van den Berg, E.H., Flores-Guerrero, J.L., Garcia, E., Connelly, M.A., de Meijer, V.E., TransplantLines Investigators, Bakker, S.J.L., Blokzijl, H., Dullaart, R.P.F., 2023. High plasma levels of betaine, a trimethylamine N-Oxide-related metabolite, are associated with the severity of cirrhosis. Liver Int 43, 424–433. https://doi.org/10.1111/liv.15310

Vergis, N., Atkinson, S.R., Knapp, S., Maurice, J., Allison, M., Austin, A., Forrest, E.H., Masson, S., McCune, A., Patch, D., Richardson, P., Gleeson, D., Ryder, S.D., Wright, M., Thursz, M.R., 2017. In Patients With Severe Alcoholic Hepatitis, Prednisolone Increases Susceptibility to Infection and Infection-Related Mortality, and Is Associated With High Circulating Levels of Bacterial DNA. Gastroenterology 152, 1068-1077.e4. https://doi.org/10.1053/j.gastro.2016.12.019

Vital, M., Rud, T., Rath, S., Pieper, D.H., Schlüter, D., 2019. Diversity of Bacteria Exhibiting Bile Acid-inducible 7α-dehydroxylation Genes in the Human Gut. Comput Struct Biotechnol J 17, 1016–1019. https://doi.org/10.1016/j.csbj.2019.07.012

Walker, B.J., Abeel, T., Shea, T., Priest, M., Abouelliel, A., Sakthikumar, S., Cuomo, C.A., Zeng, Q., Wortman, J., Young, S.K., Earl, A.M., 2014. Pilon: An Integrated Tool for Comprehensive Microbial Variant Detection and Genome Assembly Improvement. PLOS ONE 9, e112963. https://doi.org/10.1371/journal.pone.0112963

Wang, Q., Chen, C., Zuo, S., Cao, K., Li, H., 2023. Integrative analysis of the gut microbiota and faecal and serum short-chain fatty acids and tryptophan metabolites in patients with cirrhosis and hepatic encephalopathy. J Transl Med 21, 395. https://doi.org/10.1186/s12967-023-04262-9

Wick, R.R., Judd, L.M., Gorrie, C.L., Holt, K.E., 2017. Unicycler: Resolving bacterial genome assemblies from short and long sequencing reads. PLOS Computational Biology 13, e1005595. https://doi.org/10.1371/journal.pcbi.1005595

Williams, H.R.T., Cox, I.J., Walker, D.G., Cobbold, J.F.L., Taylor-Robinson, S.D., Marshall, S.E., Orchard, T.R., 2010. Differences in gut microbial metabolism are responsible for reduced hippurate synthesis in Crohn's disease. BMC Gastroenterol 10, 108. https://doi.org/10.1186/1471-230X-10-108

Wong, F., Piano, S., Singh, V., Bartoletti, M., Maiwall, R., Alessandria, C., Fernandez, J., Soares, E.C., Kim, D.J., Kim, S.E., Marino, M., Vorobioff, J., Barea, R. de C.R., Merli, M., Elkrief, L., Vargas, V., Krag, A., Singh, S.P., Lesmana, L.A., Toledo, C., Marciano, S., Verhelst, X., Intagliata, N., Rabinowich, L., Colombato, L., Kim, S.G., Gerbes, A., Durand, F., Roblero, J.P., Bruns, T., Yoon, E.L., Girala, M., Pyrsopoulos, N.T., Kim, T.H., Yim, S.Y., Juanola, A., Gadano, A., Angeli, P., International Club of Ascites Global Study Group, 2021. Clinical features and evolution of bacterial infection-related acute-on-chronic liver failure. J Hepatol 74, 330–339. https://doi.org/10.1016/j.jhep.2020.07.046

Y, Furusawa, Y, O., S, F., Ta, E., G, N., D, T., Y, N., C, U., K, K., T, K., M, Takahashi, Nn, F., S, M., E, M., S, Hino, K, A., S, O., Y, Fujimura, T, L., Jm, C., Dl, T., M, Tomita, S, Hori, O, O., T, M., H, K., J, K., K,

medRxiv preprint doi: https://doi.org/10.1101/2025.02.13.25322003; this version posted February 14, 2025. The copyright holder for this preprint (which was not certified by peer review) is the author/funder, who has granted medRxiv a license to display the preprint in perpetuity. All rights reserved. No reuse allowed without permission.

Honda, K, Hase, H, O., 2013. Commensal microbe-derived butyrate induces the differentiation of colonic regulatory T cells. Nature 504. https://doi.org/10.1038/nature12721

Zapun, A., Contreras-Martel, C., Vernet, T., 2008. Penicillin-binding proteins and beta-lactam resistance. FEMS microbiology reviews 32. https://doi.org/10.1111/j.1574-6976.2007.00095.x

Zhang, J., Kobert, K., Flouri, T., Stamatakis, A., 2014. PEAR: a fast and accurate Illumina Paired-End reAd mergeR. Bioinformatics 30, 614–620. https://doi.org/10.1093/bioinformatics/btt593

Zhang, X., Bierschenk, D., Top, J., Anastasiou, I., Bonten, M.J., Willems, R.J., van Schaik, W., 2013. Functional genomic analysis of bile salt resistance in Enterococcus faecium. BMC Genomics 14, 299. https://doi.org/10.1186/1471-2164-14-299

Zimmermann, P., Curtis, N., 2019. The effect of antibiotics on the composition of the intestinal microbiota - a systematic review. The Journal of infection 79. https://doi.org/10.1016/j.jinf.2019.10.008

Table 1: Summary of clinical characteristics of patient and healthy participant study groups (all values given as median [IQR])

Parameters			HC (n=40)	SC (n=15)	DC (n=81)	ACLF (n=57)	P value
General	Age (years)		36 (32-41)	59 (54-69)	55 (49-61)	49 (42-59)	<0.0001
	Male gender (n (%))		20 (50%)	11 (73.3%)	52 (64.2%)	36 (63.2%)	0.3287
	BMI (kg/m^2)		N/A	27.2 (23.5-32.6)	27.4 (24.0-30.5)	22.7 (20.8-23.2)	<0.0001
Aetiology of cirrhosis	Alcohol-related liver disease (n (%))		N/A	9 (60%)	57 (70.4%)	33 (57.9%)	0.2950
	Drinking /	Alcohol actively drinking (n (%))	N/A	0	12 (21%)	19 (57.6%)	0.0002

medRxiv preprint doi: https://doi.org/10.1101/2025.02.13.25322003; this version posted February 14, 2025. The copyright holder for this preprint (which was not certified by peer review) is the author/funder, who has granted medRxiv a license to display the preprint in perpetuity. All rights reserved. No reuse allowed without permission.

	Abstinent	Alcohol abstinent (n (%))	N/A	9 (100%)	45 (79%)	14 (42.4%)	
	Metabolic- dysfunction associated steatotic liver disease (MASLD) (n (%))		N/A	3 (20%)	7 (8.6%)	6 (10.5%)	0.4181
	Cholestatic/autoimmune (n (%)): Primary biliary cholangitis (PBC), primary sclerosing cholangitis (PSC), Alagille syndrome, biliary atresia, and autoimmune hepatitis (AIH).		N/A	1 (6.7%)	6 (7.4%)	11 (19.3%)	0.0832
	Metabolic (number (%)): Wilson's disease, haemochromatosis and alpha-1-antitrypsin (A1AT) deficiency		N/A	1 (6.7%)	5 (6.2%)	3 (5.3%)	0.9663
	Other (n (%)): 'Cryptogenic', treated viral hepatitis, chronic veno-occlusive related-cirrhosis (Bud Chiari), chronic porto-mesenteric venous insufficiency cirrhosis, and drug induced		N/A	1 (6.7%)	6 (7.4%)	4 (7%)	0.9928
Clinical features at enrolment	Temperature (°C)		N/A	36.5 (36.3-37.2)	36.7 (36.4-37.0)	36.5 (36.1-37.1)	0.2121
	Presence of ascites (n (%))		N/A	5 (33.3%)	58 (71.6%)	55 (96.5%)	<0.0001
	Ascites grade (n (%))	Small	N/A	5 (100%)	25 (43.1%)	35 (63.6%)	0.0107
		Moderate/ Severe	N/A	0	33 (56.9%)	20 (36.4%)	

medRxiv preprint doi: https://doi.org/10.1101/2025.02.13.25322003; this version posted February 14, 2025. The copyright holder for this preprint (which was not certified by peer review) is the author/funder, who has granted medRxiv a license to display the preprint in perpetuity. All rights reserved. No reuse allowed without permission.

	Presence of Hepatic encephalopathy (n (%))		N/A	1 (6.7%)	35 (43.2%)	49 (86%)	<0.0001
	Hepatic encephalopathy grade	1-2	N/A	1 (100%)	35 (43%)	24 (49%)	<0.0001
		3-4	N/A	0	0	25 (51%)	
	Mean arterial pressure (mmHg)		N/A	95 (87-100)	81 (76-89)	75 (70-82)	<0.0001
	Presence of bacterial infection (n (%))	Blood culture	N/A	0	2 (2.5%)	3 (5.3%)	0.4996
		Urine culture	N/A	0	5 (6.2%)	2 (3.5%)	0.5114
	Heart rate (beats per minute)		N/A	76 (65-82)	77 (60-88)	87 (78-95)	0.0010
Antibacterial therapy at enrolment (number (%))	Antibiotics – any		N/A	3 (20%)	37 (45.7%)	52 (91.2%)	<0.0001
	Antifungal – any		N/A	0	2 (2.4%)	20 (35.1%)	<0.0001
	Rifaximin		N/A	1 (6.7%)	10 (12.4%)	2 (3.5%)	0.2583
	Fluoroquinolone (Norfloxacin, Ciprofloxacin)		N/A	0	8 (9.9%)	0	0.0702
Other pharmacotherapy at enrolment (number (%))	Proton pump inhibitors (Omeprazole, Lansoprazole)		N/A	10 (66.7%)	44 (54.3%)	36 (63.2%)	0.4721
	Lactulose		N/A	2 (13.3%)	30 (37.0%)	2 (3.5%)	0.1234
	Non-selective beta-blockers (Propranolol, Carvedilol)		N/A	6 (40%)	34 (42.0%)	14 (24.6%)	0.1001

medRxiv preprint doi: https://doi.org/10.1101/2025.02.13.25322003; this version posted February 14, 2025. The copyright holder for this preprint (which was not certified by peer review) is the author/funder, who has granted medRxiv a license to display the preprint in perpetuity. All rights reserved. No reuse allowed without permission.

	H2 antagonist (Ranitidine)	N/A	0	3 (3.7%)	0	0.2567
Laboratory parameters	Haemoglobin (g/dl)	N/A	130 ± 25	112 ± 21	92 ± 15	<0.0001
	Leukocyte count (x10^9/L)	N/A	4.46 (3.96-6.11)	5.57 (4.25-7.39)	9.74 (6.54-14.57)	<0.0001
	Neutrophils (x10^9/L)	N/A	2.92 (2.14-3.69)	3.70 (2.37-5.29)	7.70 (4.85-12.21)	<0.0001
	Platelet count (x10^9/L)	N/A	111 (99-151)	106 (75-165)	86 (56-115)	0.0061
	INR	N/A	1.15 (1.10-1.29)	1.44 (1.29-1.75)	2.09 (1.69-2.93)	<0.0001
	Serum creatinine (µmol/L)	N/A	73 (66-84)	77 (57-94)	135 (87-206)	<0.0001
	Serum bilirubin (µmol/L)	N/A	20 (11-25)	41 (24-72)	209 (84-371)	<0.0001
	Albumin (g/L)	N/A	39 ± 4	33 ± 6	27 ± 7	<0.0001
	C-reactive protein (mg/L)	N/A	5.5 (2.3-11.1)	11.7 (3.4-32.9)	47.3 (23.7-70.7)	<0.0001
	Blood lactate (mmol/L)	N/A	1.4 (1.2-1.9)	1.5 (1.2-2.1)	2 (1.6-3.2)	0.0006
	Venous ammonia (µmol/L)	N/A	61 (28-88)	53 (33-72)	68 (47-107)	0.0710
Disease severity & prognostic scores	Child Pugh	N/A	6 (5-6)	8 (8-10)	12 (11-13)	<0.0001
	MELD	N/A	9 (8-11)	16 (12-23)	34 (29-39)	<0.0001

medRxiv preprint doi: https://doi.org/10.1101/2025.02.13.25322003; this version posted February 14, 2025. The copyright holder for this preprint (which was not certified by peer review) is the author/funder, who has granted medRxiv a license to display the preprint in perpetuity. All rights reserved. No reuse allowed without permission.

	UKELD	N/A	49 ± 3	55 ± 5	61 ± 6	<0.0001
	CLIF-C-AD	N/A	N/A	49 (43-53)	N/A	—
	CLIF-C-ACLF	N/A	N/A	N/A	54 (46-66)	—
	CLIF-OF	N/A	N/A	7 (6-8)	13 (11-15)	<0.0001
Transplant-free survival	30-day	N/A	0	72 (88.9%)	24 (42.1%)	<0.0001
	90-day	N/A	0	63 (77.8%))	14 (24.6%)	<0.0001

Supplementary data

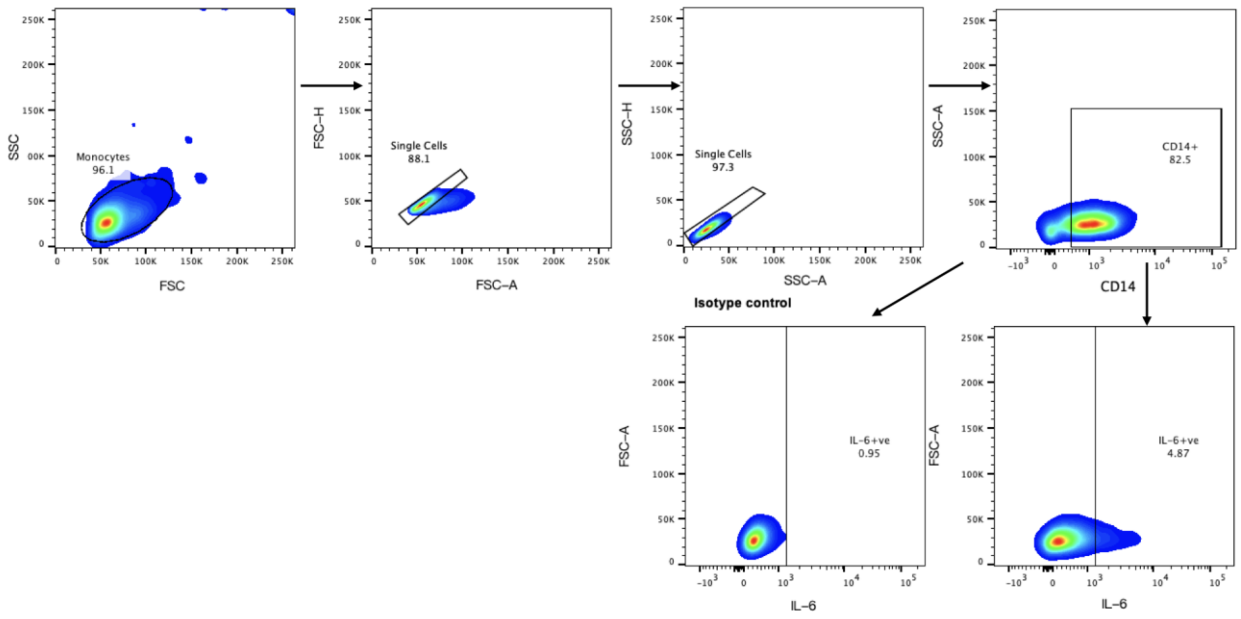

medRxiv preprint doi: https://doi.org/10.1101/2025.02.13.25322003; this version posted February 14, 2025. The copyright holder for this preprint (which was not certified by peer review) is the author/funder, who has granted medRxiv a license to display the preprint in perpetuity.
All rights reserved. No reuse allowed without permission.

Supplementary Figure 1. Representative FACS gating strategy used to identify CD14+ monocytes in peripheral blood mononuclear cells (PBMCs) with isotype control used to determine the IL-6-producing monocytes (%) in response to LPS stimulation. Side scatter (SSC), forward scatter (FSC).

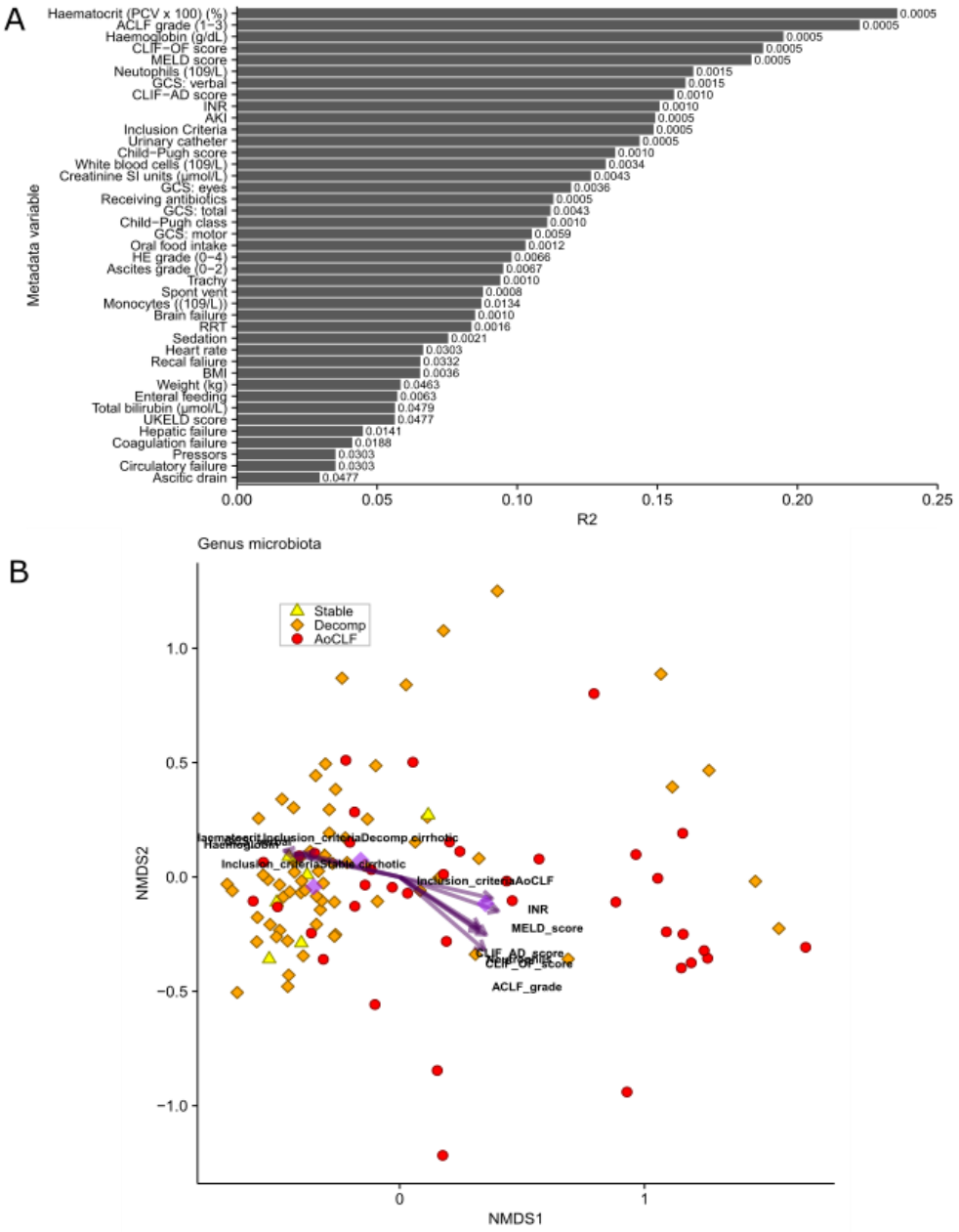

medRxiv preprint doi: https://doi.org/10.1101/2025.02.13.25322003; this version posted February 14, 2025. The copyright holder for this preprint (which was not certified by peer review) is the author/funder, who has granted medRxiv a license to display the preprint in perpetuity. All rights reserved. No reuse allowed without permission.

Supplementary Figure 2. Clinical metadata associated with cirrhosis patient gut microbiota composition.

(A) Results of envfit analysis showing clinical metadata variables significantly associated with microbiota composition after correction for multiple testing using False Discovery Rate. Bars show the R2 (squared correlation coefficient) of the correlation and numbers on bars show adjusted P-values. (B) NMDS ordination plot showing gut microbiota composition of individual liver patients with the ten clinical metadata variables with the highest R2 overlayed.

medRxiv preprint doi: https://doi.org/10.1101/2025.02.13.25322003; this version posted February 14, 2025. The copyright holder for this preprint (which was not certified by peer review) is the author/funder, who has granted medRxiv a license to display the preprint in perpetuity.
All rights reserved. No reuse allowed without permission.

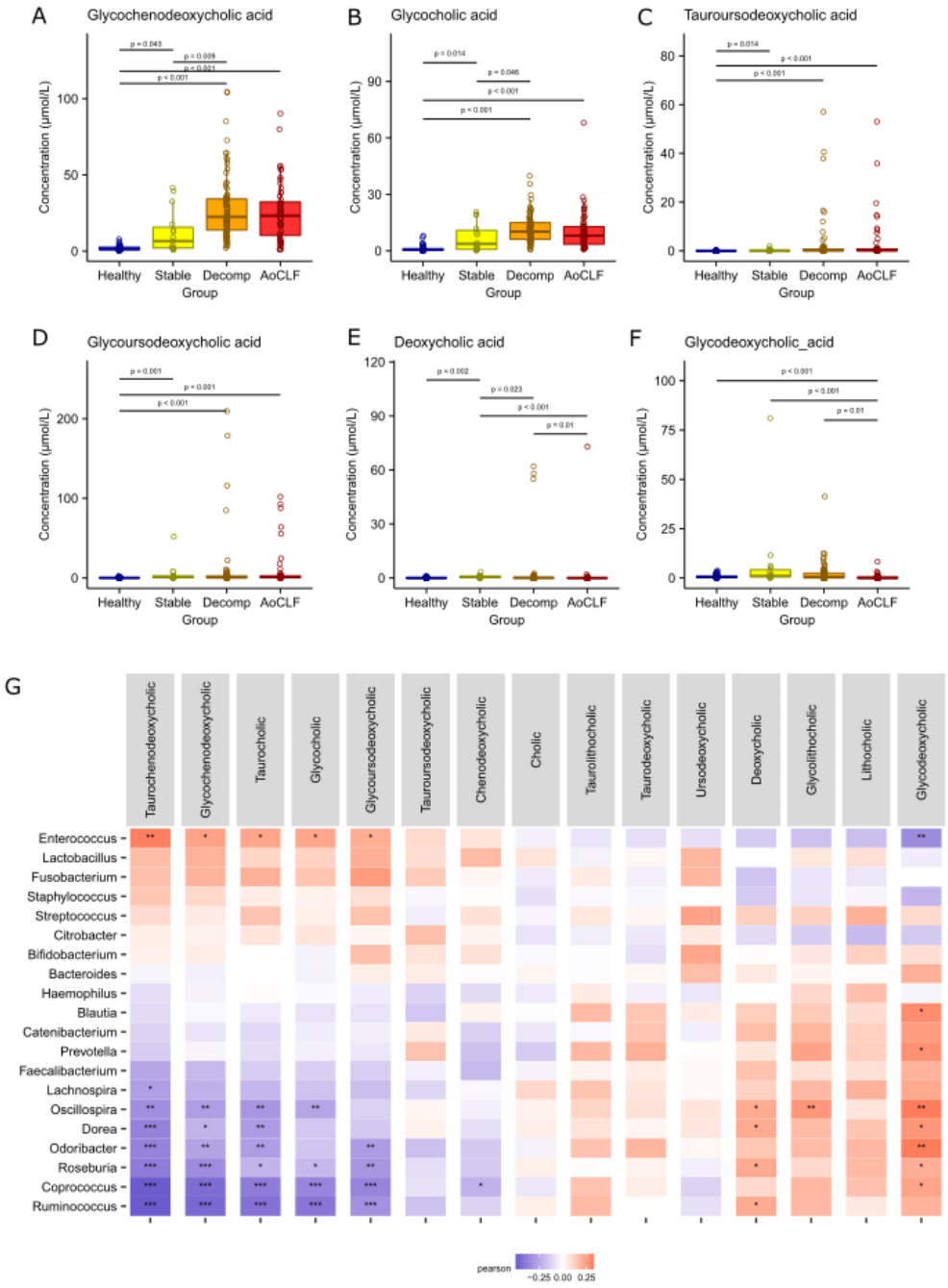

Supplementary Figure 3. Individual bile acid concentrations by cirrhosis severity and correlations between genus proportion and bile acids.

medRxiv preprint doi: https://doi.org/10.1101/2025.02.13.25322003; this version posted February 14, 2025. The copyright holder for this preprint (which was not certified by peer review) is the author/funder, who has granted medRxiv a license to display the preprint in perpetuity. All rights reserved. No reuse allowed without permission.

(A) Glycochenodeoxycholic acid, (B) Glycocholic acid, (C) Tauroursodeoxycholic acid, (D) Glycoursodeoxycholic acid, (E) Deoxycholic acid, (F) Glycodeoxycholic acid, (F) Pearson correlations between normalised plasma bile acid concentrations and normalised genus relative abundance using a Pearson correlation. P-value: * = $p<0.05$, ** = $p<0.01$, ** = $p<0.001$. Significance corrected for multiple testing.

medRxiv preprint doi: https://doi.org/10.1101/2025.02.13.25322003; this version posted February 14, 2025. The copyright holder for this preprint (which was not certified by peer review) is the author/funder, who has granted medRxiv a license to display the preprint in perpetuity. All rights reserved. No reuse allowed without permission.

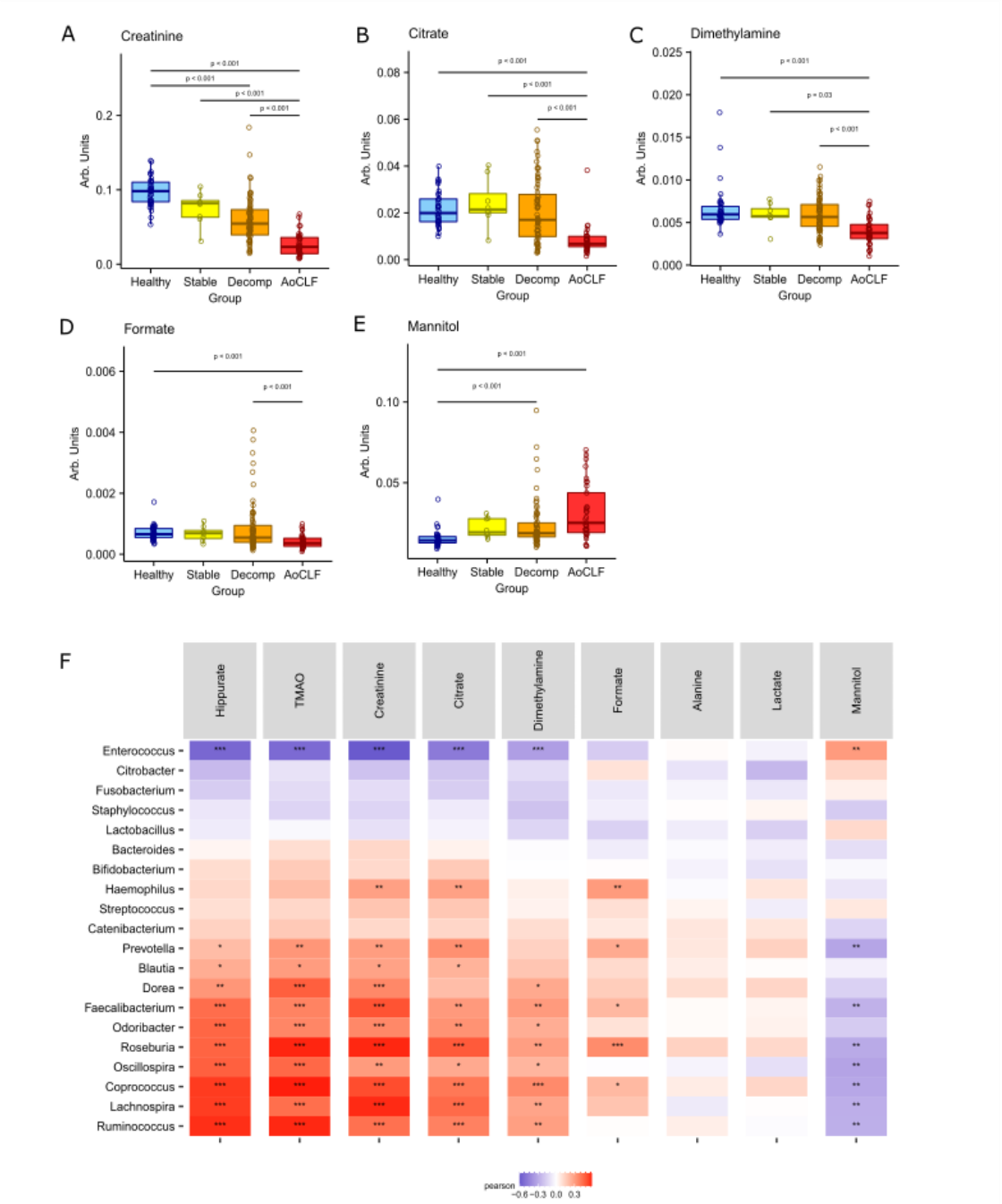

1365

1366 Supplementary Figure 4. Individual urinary metabolites by cirrhosis severity and correlations
1367 between genus proportion and plasma metabolites.

medRxiv preprint doi: https://doi.org/10.1101/2025.02.13.25322003; this version posted February 14, 2025. The copyright holder for this preprint (which was not certified by peer review) is the author/funder, who has granted medRxiv a license to display the preprint in perpetuity. All rights reserved. No reuse allowed without permission.

1368 (A) Creatinine, (B) Citrate, (C) Dimethylamine, (D) Formate, (E) Mannitol, (F) Correlations between
1369 normalised urinary metabolites and normalised genus relative abundance using a Pearson
1370 correlation. P-value: * = p<0.05, ** = p<0.01, ** = p<0.001. Significance corrected for multiple testing.

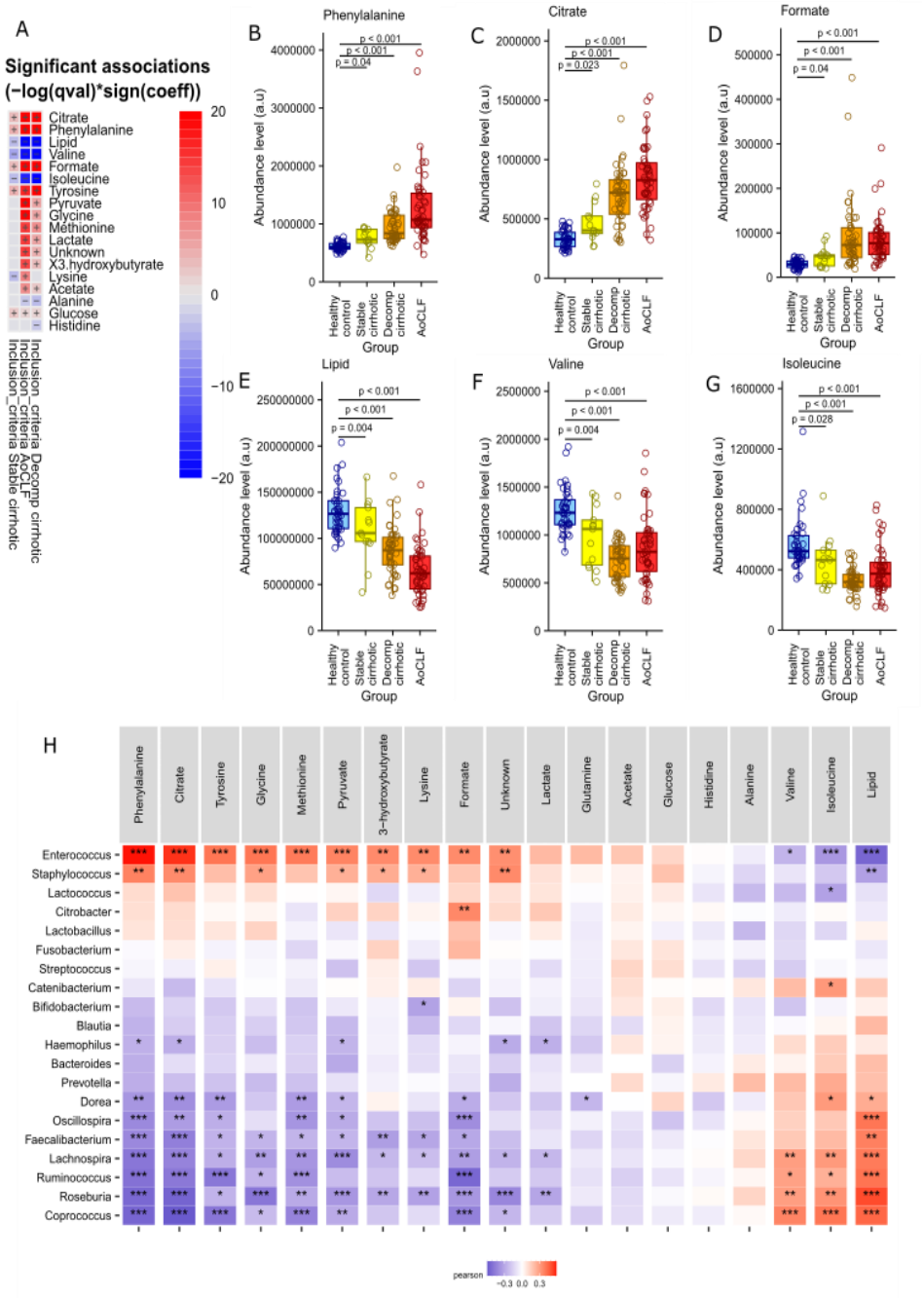

1371

medRxiv preprint doi: https://doi.org/10.1101/2025.02.13.25322003; this version posted February 14, 2025. The copyright holder for this preprint (which was not certified by peer review) is the author/funder, who has granted medRxiv a license to display the preprint in perpetuity. All rights reserved. No reuse allowed without permission.

1372 Supplementary Figure 5. Individual plasma metabolites by cirrhosis severity and correlations
1373 between genus proportion and plasma metabolites.

1374 (A) Phenylalanine, (B) Citrate, (C) Formate, (D) Lipid, (E) Valine, (F) Isoleucine, (G) Correlations
1375 between normalised plasma metabolites and normalised genus relative abundance using a Pearson
1376 correlation. P-value: * = p<0.05, ** = p<0.01, *** = p<0.001. Significance corrected for multiple
1377 testing.

1378

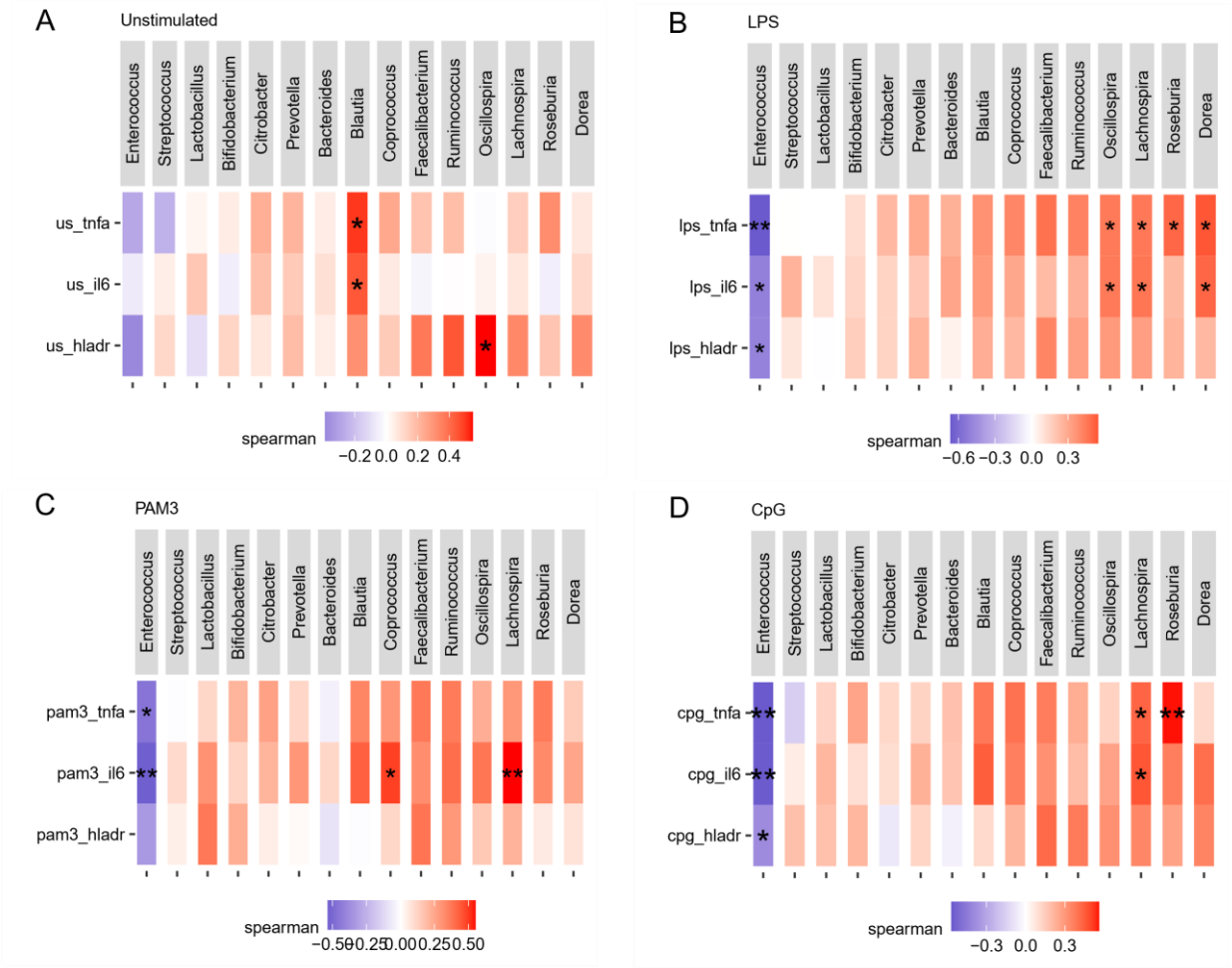

1379

medRxiv preprint doi: https://doi.org/10.1101/2025.02.13.25322003; this version posted February 14, 2025. The copyright holder for this preprint (which was not certified by peer review) is the author/funder, who has granted medRxiv a license to display the preprint in perpetuity. All rights reserved. No reuse allowed without permission.

Supplementary Figure 6. Correlations between genus proportion and monocyte stimulation.

Full correlations between the top 15 most abundant genera and TNF-alpha, IL-6, and HLA-DR percentage in (A) Unstimulated, (B) LPS stimulated, (C) PAM3 stimulated, and (D) CpG simulated monocytes. Correlations between normalised plasma metabolites and normalised genus relative abundance using a Pearson correlation. P-value: * = $p<0.05$, ** = $p<0.01$. Significance corrected for multiple testing.

medRxiv preprint doi: https://doi.org/10.1101/2025.02.13.25322003; this version posted February 14, 2025. The copyright holder for this preprint (which was not certified by peer review) is the author/funder, who has granted medRxiv a license to display the preprint in perpetuity.
All rights reserved. No reuse allowed without permission.

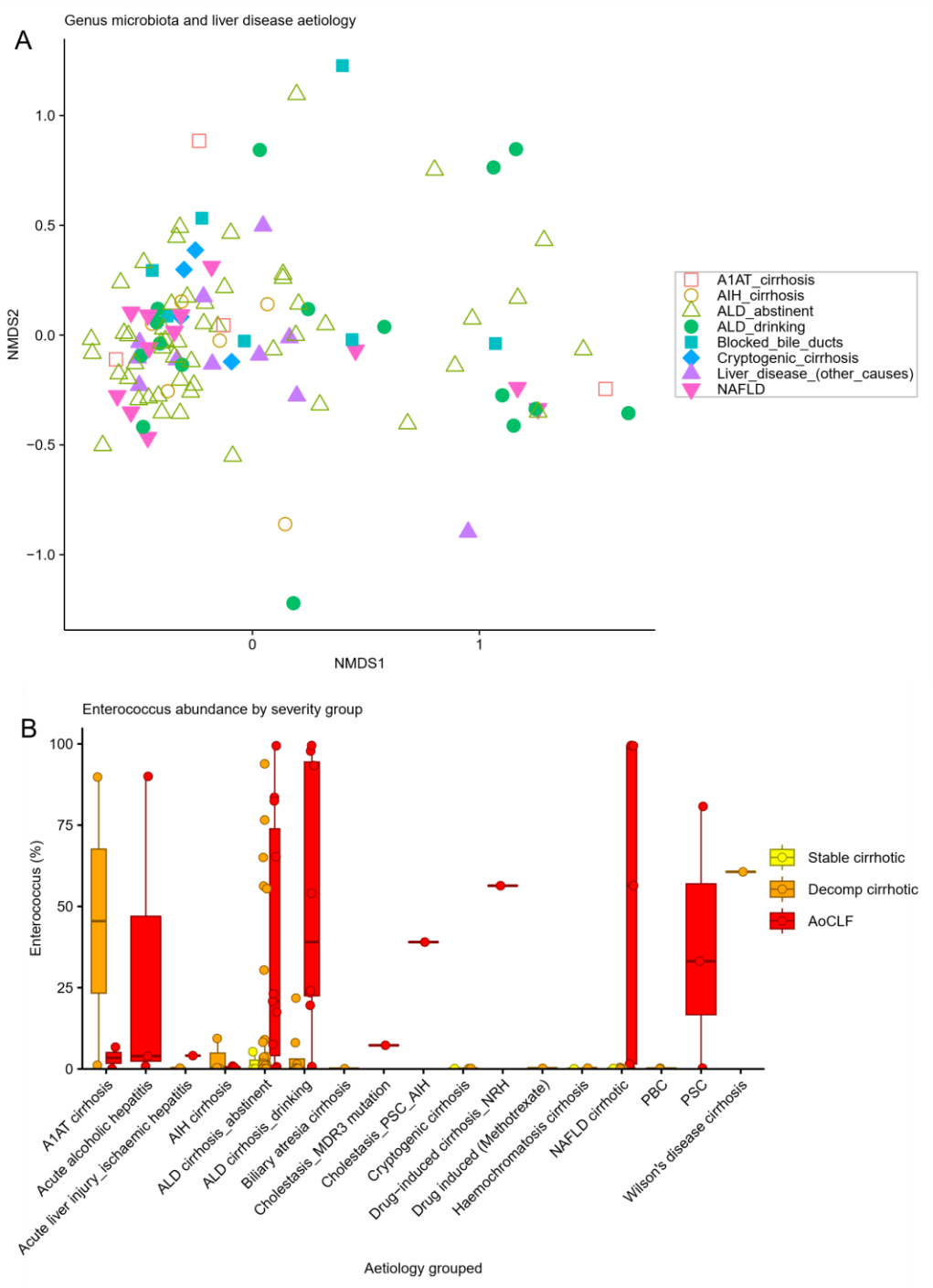

1387

1388 Supplementary Figure 7. Aetiology associations with overall microbiota composition and
1389 *Enterococcus* abundance.

medRxiv preprint doi: https://doi.org/10.1101/2025.02.13.25322003; this version posted February 14, 2025. The copyright holder for this preprint (which was not certified by peer review) is the author/funder, who has granted medRxiv a license to display the preprint in perpetuity. All rights reserved. No reuse allowed without permission.

(A) NMDS clustering of overall genus level faecal microbiota composition based on a Bray-Curtis matrix showing patient samples with patient aetiology condensed to eight groups for the purposes of analysis showing a lack of clustering by aetiology (PERMANOVA: P = 0.1). (B) Box plots show full patient aetiology groups with faecal *Enterococcus* abundance grouped by illness severity.